

# Bayesian Model Selection with Graph Structured Sparsity

Youngseok Kim and Chao Gao

*University of Chicago*

December 15, 2024

## Abstract

We propose a general algorithmic framework for Bayesian model selection. A spike-and-slab Laplacian prior is introduced to model the underlying structural assumption. Using the notion of effective resistance, we derive an EM-type algorithm with closed-form iterations to efficiently explore possible candidates for Bayesian model selection. The deterministic nature of the proposed algorithm makes it more scalable to large-scale and high-dimensional data sets compared with existing stochastic search algorithms. When applied to sparse linear regression, our framework recovers the EMVS algorithm [37] as a special case. We also discuss extensions of our framework using tools from graph algebra to incorporate complex Bayesian models such as biclustering and submatrix localization. Extensive simulation studies and real data applications are conducted to demonstrate the superior performance of our methods over its frequentist competitors such as  $\ell_0$  or  $\ell_1$  penalization.

**Keywords:** EM algorithm, graph Laplacian, sparse linear regression, clustering, bi-clustering, change-point, spike-and-slab prior

## 1 Introduction

Bayesian model selection has been an important area of research for several decades. While the general goal is to estimate the most plausible sub-model from the posterior distribution [3, 11, 36, 5] for a wide class of learning tasks, most of the developments of Bayesian model selection have been focused on variable selection in the setting of sparse linear regression [23, 29, 21, 37, 49]. One of the main challenges of Bayesian model selection is its computational efficiency. Recently, Ročková and George [37] discovered that Bayesian variable selection in sparse linear regression can be solved by an EM algorithm [10, 35] with a closed-form update at each iteration. Compared with previous stochastic search type of algorithms such as Gibbs sampling [18, 19], this deterministic alternative greatly speeds up computation for large-scale and high-dimensional data sets.

The main thrust of this paper is to develop of a general framework of Bayesian models that includes sparse linear regression, change-point detection, clustering and many other

models as special cases. We will derive a general EM-type algorithm that efficiently explores possible candidates for Bayesian model selection. When applied to sparse linear regression, our model and algorithmic frameworks naturally recover the proposal of [37]. The general framework proposed in this paper can be viewed as an algorithmic counterpart of the theoretical framework for Bayesian high-dimensional structured linear models in [16]. While the work [16] is focused on optimal posterior contraction rate and oracle inequalities, the current paper pursues a general efficient and scalable computational strategy.

In order to study various Bayesian models from a unified perspective, we introduce a spike-and-slab Laplacian prior distribution on the model parameters. The new prior distribution is an extension of the classical spike-and-slab prior [34, 18, 19] for Bayesian variable selection. Our new definition incorporates the graph Laplacian of the underlying model structure, and thus gives the name of the prior. The connection to graph algebra is an important advantage that allows us to build prior distributions for more complicated models. For example, using graph products such as Cartesian product or Kronecker product [25, 28], we can construct prior distributions for biclustering models from the Laplacian of the graph products of row and column clustering structures. This leads to great flexibility in analyzing real data sets of complex structures.

The derivation of the EM algorithm under our general framework is a nontrivial task. When the underlying base graph of the model structure is a tree, the derivation of the EM algorithm is straightforward by following the arguments in [37]. However, for a general base graph that is not a tree, the arguments in [37] do not apply. To overcome this difficulty, we introduce a relaxation through the concept of effective resistance [31, 20, 42] that adapts to the underlying graphical structure of the model. The lower bound given by this relaxation is then used to derive an EM-type algorithm that works under the general framework.

The rest of the paper is organized as follows. In Section 2, we introduce the general framework of Bayesian models and discuss the spike-and-slab Laplacian prior. The EM algorithm will be derived in Section 3 for both the case of trees and general base graphs. In Section 4, we discuss how to incorporate latent variables and propose a new Bayesian clustering models under our framework. Section 5 introduces the techniques of graph products and several important extensions of our framework. We will also discuss a non-Gaussian spike-and-slab Laplacian prior in Section 6 with a natural application to reduced isotonic regression [38]. Finally, extensive simulated and real data analysis will be presented in Section 7.

## 2 A General Framework of Bayesian Models

In this section, we describe a general framework for building Bayesian structured models on graphs. To be specific, the prior structural assumption on the parameter  $\theta \in \mathbb{R}^p$  will be encoded by a graph. Throughout the paper,  $G = (V, E)$  is an undirected graph with  $V = [p]$  and some  $E \subset \{(i, j) : 1 \leq i < j \leq p\}$ . It is referred to as the *base graph* of the model, and our goal is to learn a sparse subgraph of  $G$  from the data. We use  $p = |V|$  and  $m = |E|$  for the node size and edge size of the base graph.

## 2.1 Model Description

We start with the Gaussian linear model  $y|\beta, \sigma^2 \sim N(X\beta, \sigma^2 I_n)$  that models an  $n$ -dimensional observation. The design matrix  $X \in \mathbb{R}^{n \times p}$  is determined by the context of the problem. Given some nonzero vector  $w \in \mathbb{R}^p$ , the Euclidean space  $\mathbb{R}^p$  can be decomposed as a direct sum of the one-dimensional subspace spanned by  $w$  and its orthogonal complement. In other words, we can write

$$\beta = \frac{1}{\|w\|^2} w w^T \beta + \left( I_p - \frac{1}{\|w\|^2} w w^T \right) \beta.$$

The structural assumption will be imposed by a prior on the second term above. To simply notation, we introduce the space  $\Theta_w = \{\theta \in \mathbb{R}^p : w^T \theta = 0\}$ . Then, any  $\beta \in \mathbb{R}^p$  can be decomposed as  $\beta = \alpha w + \theta$  for some  $\alpha \in \mathbb{R}$  and  $\theta \in \Theta_w$ . The likelihood is thus given by

$$y|\alpha, \theta, \sigma^2 \sim N(X(\alpha w + \theta), \sigma^2 I_n). \quad (1)$$

The prior distribution on the vector  $\alpha w + \theta$  will be specified by independent priors on  $\alpha$  and  $\theta$ . They are given by

$$\alpha|\sigma^2 \sim N(0, \sigma^2/\nu), \quad (2)$$

$$\theta|\gamma, \sigma^2 \sim p(\theta|\gamma, \sigma^2) \propto \prod_{(i,j) \in E} \exp\left(-\frac{(\theta_i - \theta_j)^2}{2\sigma^2[v_0\gamma_{ij} + v_1(1 - \gamma_{ij})]}\right) \mathbb{I}\{\theta \in \Theta_w\}. \quad (3)$$

Under the prior distribution,  $\alpha$  is centered at 0 and has precision  $\nu/\sigma^2$ . The parameter  $\theta$  is modeled by a prior distribution on  $\Theta_w$  that encodes a pairwise relation between  $\theta_i$  and  $\theta_j$ . Here,  $v_0$  is a very small scalar and  $v_1$  is a very large scalar. For a pair  $(i, j) \in E$  in the base graph, the prior enforces the closeness between  $\theta_i$  and  $\theta_j$  when  $\gamma_{ij} = 1$ . Our goal is then to learn the most probable subgraph structure encoded by  $\{\gamma_{ij}\}$ , which will be estimated from the posterior distribution.

We finish the Bayesian modeling by putting priors on  $\gamma$  and  $\sigma^2$ . They are given by

$$\gamma|\eta \sim p(\gamma|\eta) \propto \prod_{(i,j) \in E} \eta^{\gamma_{ij}} (1 - \eta)^{1 - \gamma_{ij}} \mathbb{I}\{\gamma \in \Gamma\}, \quad (4)$$

$$\eta \sim \text{Beta}(A, B), \quad (5)$$

$$\sigma^2 \sim \text{InvGamma}(a/2, b/2). \quad (6)$$

Besides the standard conjugate priors on  $\eta$  and  $\sigma^2$ , the independent Bernoulli prior on  $\gamma$  is restricted on a set  $\Gamma \subset \{0, 1\}^m$ . This restriction is sometimes useful for particular models, but for now we assume that  $\Gamma = \{0, 1\}^m$  until it is needed in Section 4.

The Bayesian model is now fully specified. The joint distribution is

$$p(y, \alpha, \theta, \gamma, \eta, \sigma^2) = p(y|\alpha, \theta, \sigma^2) p(\alpha|\sigma^2) p(\theta|\gamma, \sigma^2) p(\gamma|\eta) p(\eta) p(\sigma^2). \quad (7)$$

Among these distributions, the most important one is  $p(\theta|\gamma, \sigma^2)$ . To understand its properties, we introduce the *incidence matrix*  $D \in \mathbb{R}^{m \times p}$  for the base graph  $G = (V, E)$ . The matrix

$D$  has entries  $D_{ei} = 1$  and  $D_{ej} = -1$  if  $e = (i, j)$ , and  $D_{ek=0}$  if  $k \neq i, j$ . We note that the definition of  $D$  depends on the order of edges  $\{(i, j)\}$  even if  $G$  is an unordered graph. However, this does not affect any application that we will need in the paper. We then define the Laplacian matrix

$$L_\gamma = D^T \text{diag} (v_0^{-1}\gamma + v_1^{-1}(1 - \gamma)) D.$$

It is easy to see that  $L_\gamma$  is the graph Laplacian of the weighted graph with adjacency matrix  $\{v_0^{-1}\gamma_{ij} + v_1^{-1}(1 - \gamma_{ij})\}$ . Thus, we can write (3) as

$$p(\theta|\gamma, \sigma^2) \propto \exp \left( -\frac{1}{2\sigma^2} \theta^T L_\gamma \theta \right) \mathbb{I}\{\theta \in \Theta_w\}. \quad (8)$$

Given its form, we name (8) the *spike-and-slab Laplacian prior*.

**Proposition 2.1.** *Suppose  $G = (V, E)$  is a connected base graph. For any  $\gamma \in \{0, 1\}^m$  and  $v_0, v_1 \in (0, \infty)$ , the graph Laplacian  $L_\gamma$  is positive semi-definite and has rank  $p - 1$ . The only eigenvector corresponding to its zero eigenvalue is proportional to  $\mathbf{1}_p$ , the vector with all entries 1. As a consequence, as long as  $\mathbf{1}_p^T w \neq 0$ , the spike-and-slab Laplacian prior is a non-degenerate distribution on  $\Theta_w$ . Its density function with respect to the Lebesgue measure restricted to  $\Theta_w$  is*

$$p(\theta|\gamma, \sigma^2) = \frac{1}{(2\pi\sigma^2)^{(p-1)/2}} \sqrt{\det_w(L_\gamma)} \exp \left( -\frac{1}{2\sigma^2} \theta^T L_\gamma \theta \right) \mathbb{I}\{\theta \in \Theta_w\},$$

where  $\det_w(L_\gamma)$  is the product of all nonzero eigenvalues of the positive semi-definite matrix  $\left(I_p - \frac{1}{\|w\|^2} w w^T\right) L_\gamma \left(I_p - \frac{1}{\|w\|^2} w w^T\right)$ .

The proposition reveals two important conditions that lead to the well-definedness of the spike-and-slab Laplacian prior: the connectedness of the base graph  $G = (V, E)$  and  $\mathbf{1}_p^T w \neq 0$ . Without either condition, the distribution would be degenerate on  $\Theta_w$ . Extensions to a base graph that is not necessarily connected is possible. We leave this task to Section 4 and Section 5, where tools from graph algebra are introduced.

## 2.2 Examples

The Bayesian model (7) provides a very general framework. By choosing a different base graph  $G = (V, E)$ , a design matrix  $X$ , a grounding vector  $w \in \mathbb{R}^p$  and a precision parameter  $\nu$ , we then obtain a different model. Several important examples are given below.

**Example 2.1** (Sparse linear regression). *The sparse linear regression model  $y|\theta, \sigma^2 \sim N(X\theta, \sigma^2 I_n)$  is a special case of (1). To put it into the general framework, we can expand the design matrix  $X \in \mathbb{R}^{n \times p}$  and the regression vector  $\theta \in \mathbb{R}^p$  by  $[0_n, X] \in \mathbb{R}^{n \times (p+1)}$  and  $[\theta_0; \theta] \in \mathbb{R}^{p+1}$ . With the grounding vector  $w = [1; 0_p]$ , the sparse linear regression model can be recovered from (1). For the prior distribution, the base graph  $G$  consists of nodes  $V = \{0, 1, \dots, p\}$  and edges*

$\{(0, i) : i \in [p]\}$ . We set  $\nu = \infty$ , so that  $\theta_0 = 0$  with prior probability one. Then, (3) is reduced to

$$\theta|\gamma, \sigma^2 \sim p(\theta|\gamma, \sigma^2) \propto \prod_{i=1}^p \exp\left(-\frac{\theta_i^2}{2\sigma^2[v_0\gamma_{0i} + v_1(1 - \gamma_{0i})]}\right).$$

That is,  $\theta_i|\gamma, \sigma^2 \sim N(0, \sigma^2[v_0\gamma_{0i} + v_1(1 - \gamma_{0i})])$  independently for all  $i \in [n]$ . This is recognized as the spike-and-slab Gaussian prior for Bayesian sparse linear regression considered by [18, 19, 37].

**Example 2.2** (Change-point detection). Set  $n = p$ ,  $X = I_n$ , and  $w = \mathbf{1}_n$ . We then have  $y_i|\theta, \sigma^2 \sim N(\alpha + \theta_i, \sigma^2)$  independently for all  $i \in [n]$  from (1). For the prior distribution on  $\alpha$  and  $\theta$ , we consider  $\nu = 0$  and a one-dimensional chain graph  $G = (V, E)$  with  $E = \{(i, i+1) : i \in [n-1]\}$ . This leads to a flat prior on  $\alpha$ , and the prior on  $\theta$  is given by

$$\theta|\gamma, \sigma^2 \sim p(\theta|\gamma, \sigma^2) \propto \prod_{i=1}^{n-1} \exp\left(-\frac{(\theta_i - \theta_{i+1})^2}{2\sigma^2[v_0\gamma_{i,i+1} + v_1(1 - \gamma_{i,i+1})]}\right) \mathbb{I}\{\mathbf{1}_p^T \theta = 0\}.$$

A more general change-point model on a tree can also be obtained by constructing a tree base graph  $G$ .

**Example 2.3** (Two-dimensional image denoising). Consider a rectangular set of observations  $y \in \mathbb{R}^{n_1 \times n_2}$ . With the same construction in Example 2.2 applied to  $\text{vec}(y)$ , we obtain  $y_{ij}|\theta, \sigma^2 \sim N(\alpha + \theta_{ij}, \sigma^2)$  independently for all  $(i, j) \in [n_1] \times [n_2]$  from (1). To model images, we consider a prior distribution that imposes closeness to nearby pixels. Consider  $\nu = 0$  and a base graph  $G = (V, E)$  shown in the picture below.

$$\begin{array}{cccc} \theta_{11} & - & \theta_{12} & - \cdots - & \theta_{1n_2} \\ | & & | & & | \\ \theta_{21} & - & \theta_{22} & - \cdots - & \theta_{2n_2} \\ | & & | & & | \\ \vdots & - & \vdots & - & \vdots \\ | & & | & & | \\ \theta_{n_11} & - & \theta_{n_12} & - \cdots - & \theta_{n_1n_2} \end{array}$$

We then obtain a flat prior on  $\alpha$ , and

$$\theta|\gamma, \sigma^2 \sim p(\theta|\gamma, \sigma^2) \propto \prod_{(ik,jl) \in E} \exp\left(-\frac{(\theta_{ik} - \theta_{jl})^2}{2\sigma^2[v_0\gamma_{ik,jl} + v_1(1 - \gamma_{ik,jl})]}\right) \mathbb{I}\{\mathbf{1}_{n_1}^T \theta \mathbf{1}_{n_2} = 0\}.$$

Note that  $G$  is not a tree in this case.

### 3 EM Algorithm

In this section, we will develop efficient EM algorithms for the general model. It turns out that the bottleneck is the computation of  $\det_w(L_\gamma)$  given some  $\gamma \in \{0, 1\}^m$ .

**Lemma 3.1.** *Let  $\text{spt}(G)$  be the set of all spanning trees of  $G$ . Then*

$$\det_w(L_\gamma) = \frac{(\mathbf{1}_p^T w)^2}{\|w\|^2} \sum_{T \in \text{spt}(G)} \prod_{(i,j) \in T} [v_0^{-1} \gamma_{ij} + v_1^{-1} (1 - \gamma_{ij})].$$

*In particular, if  $G$  is a tree, then  $\det_w(L_\gamma) = \frac{(\mathbf{1}_p^T w)^2}{\|w\|^2} \prod_{(i,j) \in E} [v_0^{-1} \gamma_{ij} + v_1^{-1} (1 - \gamma_{ij})]$ .*

The lemma suggests that the hardness of computing  $\det_w(L_\gamma)$  depends on the number of spanning trees of the base graph  $G$ . When the base graph is a tree,  $\det_w(L_\gamma)$  is factorized over the edges of the tree, which greatly simplifies the derivation of the algorithm. We will derive a closed-form EM algorithm in Section 3.1 when  $G$  is a tree, and the algorithm for a general  $G$  will be given in Section 3.2.

### 3.1 The Case of Trees

We treat  $\gamma$  as latent. Our goal is to maximize the marginal distribution after integrating out the latent variables. That is,

$$\max_{\alpha, \theta \in \Theta_w, \eta, \sigma^2} \log \sum_{\gamma} p(y, \alpha, \theta, \gamma, \eta, \sigma^2), \quad (9)$$

where  $p(y, \alpha, \theta, \gamma, \eta, \sigma^2)$  is given by (7). Since the summation over  $\gamma$  is intractable, we consider an equivalent form of (9), which is

$$\max_q \max_{\alpha, \theta \in \Theta_w, \eta, \sigma^2} \sum_{\gamma} q(\gamma) \log \frac{p(y, \alpha, \theta, \gamma, \eta, \sigma^2)}{q(\gamma)}. \quad (10)$$

Then, the EM algorithm is equivalent to iteratively updating  $q, \alpha, \theta \in \Theta_w, \eta, \sigma^2$  [35].

Now we illustrate the EM algorithm that solves (10). The E-step is to update  $q(\gamma)$  given the previous values of  $\theta, \eta, \sigma$ . In view of (7), we have

$$q^{\text{new}}(\gamma) \propto p(y, \alpha, \theta, \gamma, \eta, \sigma^2) \propto p(\theta|\gamma, \sigma^2) p(\gamma|\eta). \quad (11)$$

According to (3.1),  $p(\theta|\gamma, \sigma^2)$  can be factorized when the base graph  $G = (V, E)$  is a tree. Therefore, with a simpler notation  $q_{ij} = q(\gamma_{ij} = 1)$ , we have  $q^{\text{new}}(\gamma) = \prod_{(i,j) \in E} (q_{ij}^{\text{new}})^{\gamma_{ij}} (1 - q_{ij}^{\text{new}})^{1 - \gamma_{ij}}$ , where

$$q_{ij}^{\text{new}} = \frac{\eta \phi(\theta_i - \theta_j; 0, \sigma^2 v_0)}{\eta \phi(\theta_i - \theta_j; 0, \sigma^2 v_0) + (1 - \eta) \phi(\theta_i - \theta_j; 0, \sigma^2 v_1)}. \quad (12)$$

Here,  $\phi(\cdot; \mu, \sigma^2)$  stands for the density function of  $N(\mu, \sigma^2)$ .

To derive the M-step, we introduce the following function

$$F(\alpha, \theta; q) = \|y - X(\alpha w + \theta)\|^2 + \nu \alpha^2 + \theta^T L_q \theta, \quad (13)$$

where  $L_q$  is obtained by replacing  $\gamma$  with  $q$  in the definition of the graph Laplacian  $L_\gamma$ . The M-step consists of the following three updates,

$$(\alpha^{\text{new}}, \theta^{\text{new}}) = \underset{\alpha, \theta \in \Theta_w}{\operatorname{argmin}} F(\alpha, \theta; q^{\text{new}}), \quad (14)$$

$$(\sigma^2)^{\text{new}} = \underset{\sigma^2}{\operatorname{argmin}} \left[ \frac{F(\alpha^{\text{new}}, \theta^{\text{new}}; q^{\text{new}}) + b}{2\sigma^2} + \frac{p + n + a + 2}{2} \log(\sigma^2) \right], \quad (15)$$

$$\eta^{\text{new}} = \underset{\eta}{\operatorname{argmax}} [(A - 1 + q_{\text{sum}}^{\text{new}}) \log \eta + (B - 1 + p - 1 - q_{\text{sum}}^{\text{new}}) \log(1 - \eta)], \quad (16)$$

where the notation  $q_{\text{sum}}^{\text{new}}$  stands for  $\sum_{(i,j) \in E} q_{ij}^{\text{new}}$ . While (14) is a simple quadratic programming, (15) and (16) have closed forms, which are given by

$$(\sigma^2)^{\text{new}} = \frac{F(\alpha^{\text{new}}, \theta^{\text{new}}; q^{\text{new}}) + b}{p + n + a + 2} \quad \text{and} \quad \eta^{\text{new}} = \frac{A - 1 + q_{\text{sum}}^{\text{new}}}{A + B + p - 3}. \quad (17)$$

We remark that the EMVS algorithm [37] is a special case for the sparse linear regression problem discussed in Example 2.1.

### 3.2 General Graphs

When the base graph  $G$  is not a tree, the E-step becomes computationally infeasible due to the lack of separability of  $p(\theta|\gamma, \sigma^2)$  in  $\gamma$ . In fact, given the form of the density function in Proposition 2.1, the main problem lies in the term  $\sqrt{\det_w(L_\gamma)}$ , which cannot be factorized over  $(i, j) \in E$  when the base graph  $G = (V, E)$  is not a tree (Lemma 3.1). To overcome the difficulty, we consider optimizing a lower bound of the objective function (10). This means we need to find a good lower bound for  $\log \det_w(L_\gamma)$ . Similar techniques are also advocated in the context of learning exponential family graphical models [48].

By Lemma 3.1, we can write

$$\log \det_w(L_\gamma) = \log \sum_{T \in \text{spt}(G)} \prod_{(i,j) \in T} [v_0^{-1} \gamma_{ij} + v_1^{-1} (1 - \gamma_{ij})] + \log \frac{(\mathbb{1}_p^T w)^2}{\|w\|^2}.$$

We only need to lower bound the first term on the right hand side of the equation above, because the second term is independent of  $\gamma$ . By Jensen's inequality, for any non-negative sequence  $\{\lambda(T)\}_{T \in \text{spt}(G)}$  such that  $\sum_{T \in \text{spt}(G)} \lambda(T) = 1$ , we have

$$\begin{aligned} & \log \sum_{T \in \text{spt}(G)} \prod_{(i,j) \in T} [v_0^{-1} \gamma_{ij} + v_1^{-1} (1 - \gamma_{ij})] \\ & \geq \sum_{T \in \text{spt}(G)} \lambda(T) \log \prod_{(i,j) \in T} [v_0^{-1} \gamma_{ij} + v_1^{-1} (1 - \gamma_{ij})] - \sum_{T \in \text{spt}(G)} \lambda(T) \log \lambda(T) \\ & = \sum_{(i,j) \in E} \left( \sum_{T \in \text{spt}(G)} \lambda(T) \mathbb{I}\{(i,j) \in T\} \right) \log [v_0^{-1} \gamma_{ij} + v_1^{-1} (1 - \gamma_{ij})] - \sum_{T \in \text{spt}(G)} \lambda(T) \log \lambda(T). \end{aligned}$$

One of the most natural choices of the weights  $\{\lambda(T)\}_{T \in \text{spt}(G)}$  is the uniform distribution

$$\lambda(T) = \frac{1}{|\text{spt}(G)|}.$$

This leads to the following lower bound

$$\begin{aligned} & \log \sum_{T \in \text{spt}(G)} \prod_{(i,j) \in T} [v_0^{-1} \gamma_{ij} + v_1^{-1} (1 - \gamma_{ij})] \\ & \geq \sum_{(i,j) \in E} r_{ij} \log [v_0^{-1} \gamma_{ij} + v_1^{-1} (1 - \gamma_{ij})] + \log |\text{spt}(G)|, \end{aligned} \quad (18)$$

where

$$r_{ij} = \frac{1}{|\text{spt}(G)|} \sum_{T \in \text{spt}(G)} \mathbb{I}\{(i,j) \in T\}. \quad (19)$$

The quantity  $r_{ij}$  defined in (19) is recognized as the *effective resistance* between the  $i$ th and the  $j$ th nodes [31, 20]. Given a graph, we can treat each edge as a resistor with resistance 1. Then, the effective resistance between the  $i$ th and the  $j$ th nodes is the resistance between  $i$  and  $j$  given by the whole graph. That is, if we treat the entire graph as a resistor. Let  $L$  be the (unweighted) Laplacian matrix of the base graph  $G = (V, E)$ , and  $L^+$  its pseudo-inverse. Then, an equivalent definition of (19) is given by the formula

$$r_{ij} = (e_i - e_j)^T L^+ (e_i - e_j),$$

where  $e_j$  is the basis vector with the  $j$ th entry 1 and the remaining entries 0. Therefore, computation of the effective resistance can leverage fast Laplacian solvers in the literature [43, 30]. Some important examples of effective resistance are listed below:

- When  $G$  is the complete graph of size  $p$ , then  $r_{ij} = 2/p$  for all  $(i,j) \in E$ .
- When  $G$  is the complete bipartite graph of sizes  $p$  and  $k$ , then  $r_{ij} = \frac{p+k-1}{pk}$  for all  $(i,j) \in E$ .
- When  $G$  is a tree, then  $r_{ij} = 1$  for all  $(i,j) \in E$ .
- When  $G$  is a two-dimensional grid graph of size  $n_1 \times n_2$ , then  $r_{ij} \in [0.5, 0.75]$  depending on how close the edge  $(i,j)$  is from its closest corner.
- When  $G$  is a lollipop graph, the conjunction of a linear chain with size  $p$  and a complete graph with size  $k$ , then  $r_{ij} = 1$  or  $2/k$  depending on whether the edge  $(i,j)$  belongs to the chain or the complete graph.

By (18), we obtain the following lower bound for the objective function (10),

$$\max_q \max_{\alpha, \theta \in \Theta_{w, \eta, \sigma^2}} \sum_{\gamma} q(\gamma) \log \frac{p(y|\alpha, \theta, \sigma^2) p(\alpha|\sigma^2) \tilde{p}(\theta|\gamma, \sigma^2) p(\gamma|\eta) p(\eta) p(\sigma^2)}{q(\gamma)}, \quad (20)$$

where the formula of  $\tilde{p}(\theta|\gamma, \sigma^2)$  is obtained by applying the lower bound (18) in the formula of  $p(\theta|\gamma, \sigma^2)$  in Proposition 2.1. Since  $\tilde{p}(\theta|\gamma, \sigma^2)$  can be factorized over  $(i, j) \in E$ , the E-step is given by  $q^{\text{new}}(\gamma) = \prod_{(i,j) \in E} (q_{ij}^{\text{new}})^{\gamma_{ij}} (1 - q_{ij}^{\text{new}})^{1-\gamma_{ij}}$ , where

$$q_{ij}^{\text{new}} = \frac{\eta v_0^{-\frac{r_{ij}}{2}} e^{-\frac{1}{2\sigma^2 v_0}(\theta_i - \theta_j)^2}}{\eta v_0^{-\frac{r_{ij}}{2}} e^{-\frac{1}{2\sigma^2 v_0}(\theta_i - \theta_j)^2} + (1 - \eta) v_1^{-\frac{r_{ij}}{2}} e^{-\frac{1}{2\sigma^2 v_1}(\theta_i - \theta_j)^2}}. \quad (21)$$

Observe that the lower bound (18) is independent of  $\alpha, \theta, \eta, \sigma^2$ , and thus the M-step remains the same as in the case of a tree base graph. The formulas are given by (14)-(16), except that (16) needs to be replaced by

$$\eta^{\text{new}} = \frac{A - 1 + q_{\text{sum}}^{\text{new}}}{A + B + m - 2}.$$

The EM algorithm for a general base graph can be viewed as a natural extension of that of a tree base graph. When  $G = (V, E)$  is a tree, it is easy to see from the formula (19) that  $r_{ij} = 1$  for all  $(i, j) \in E$ . In this case, the E-step (21) is reduced to (12), and the inequality (18) becomes an equality.

### 3.3 Bayesian Model Selection

The output of the EM algorithm  $\hat{q}(\gamma)$  can be understood as an estimator of the posterior distribution  $p(\gamma|\hat{\alpha}, \hat{\theta}, \hat{\sigma}^2, \hat{\eta})$ , where  $\hat{\alpha}, \hat{\theta}, \hat{\sigma}^2, \hat{\eta}$  are obtained from the M-step. Then, we get a subgraph according to the thresholding rule  $\hat{\gamma}_{ij} = \mathbb{I}\{\hat{q}_{ij} \geq 1/2\}$ . It can be understood as a model learned from the data. The sparsity of the model critically depends on the values of  $v_0$  and  $v_1$  in the spike-and-slab Laplacian prior. With a fixed large value of  $v_1$ , we can obtain the solution path of  $\hat{\gamma} = \hat{\gamma}(v_0)$  by varying  $v_0$  from 0 to  $v_1$ . The question then is how to select the best model along the solution path of the EM algorithm.

The strategy suggested by [37] is to calculate the posterior score  $p(\gamma|y)$  with respect to the Bayesian model of  $v_0 = 0$ . While the meaning of  $p(\gamma|y)$  corresponding to  $v_0 = 0$  is easily understood for the sparse linear regression setting in [37], it is less clear for a general base graph  $G = (V, E)$ .

In order to define a version of (7) for  $v_0 = 0$ , we need to introduce the concept of *edge contraction*. Given a  $\gamma \in \{0, 1\}^m$ , the graph corresponding to the adjacency matrix  $\gamma$  induces a partition of disconnected components  $\{\mathcal{C}_1, \dots, \mathcal{C}_s\}$  of  $[p]$ . In other words,  $\{i, j\} \subset \mathcal{C}_l$  for some  $l \in [s]$  if and only if there is some path between  $i$  and  $j$  in the graph  $\gamma$ . For notational convenience, we define a vector  $z \in [s]^n$  so that  $z_i = l$  if and only if  $i \in \mathcal{C}_l$ . A membership matrix  $Z_\gamma \in \{0, 1\}^{p \times s}$  is defined with its  $(i, l)$ th entry being the indicator  $\mathbb{I}\{z_i = l\}$ .

We let  $\tilde{G} = (\tilde{V}, \tilde{E})$  be a graph obtained from the base graph  $G = (V, E)$  after the operation of edge contraction. In other words, every node in  $\tilde{G}$  is obtained by combining nodes in  $G$  according to the partition of  $\{\mathcal{C}_1, \dots, \mathcal{C}_s\}$ . To be specific,  $\tilde{V} = [s]$ , and  $(k, l) \in \tilde{E}$  if and only if there exists some  $i \in \mathcal{C}_k$  and some  $j \in \mathcal{C}_l$  such that  $(i, j) \in E$ .

Now we are ready to define a limiting version of (3) as  $v_0 \rightarrow 0$ . Let  $\tilde{L}_\gamma = D^T \text{diag}(v_1^{-1}(1 - \gamma))D$ , which is the graph Laplacian of the weighted graph with adjacency matrix  $\{v_1^{-1}(1 - \gamma_{ij})\}$ . Then, define

$$p(\tilde{\theta}|\gamma, \sigma^2) = \frac{1}{(2\pi\sigma^2)^{(s-1)/2}} \sqrt{\det_{Z_\gamma^T w}(Z_\gamma^T \tilde{L}_\gamma Z_\gamma)} \exp\left(-\frac{\tilde{\theta}^T Z_\gamma^T \tilde{L}_\gamma Z_\gamma \tilde{\theta}}{2\sigma^2}\right) \mathbb{I}\{\tilde{\theta} \in \Theta_{Z_\gamma^T w}\}. \quad (22)$$

With  $\tilde{G} = (\tilde{V}, \tilde{E})$  standing for the contracted base graph, the prior distribution (22) can also be written as

$$p(\tilde{\theta}|\gamma, \sigma^2) \propto \exp\left(-\sum_{(k,l) \in \tilde{E}} \frac{\omega_{kl}(\tilde{\theta}_k - \tilde{\theta}_l)^2}{2\sigma^2 v_1}\right) \mathbb{I}\{\tilde{\theta} \in \Theta_{Z_\gamma^T w}\}, \quad (23)$$

where  $\omega_{kl} = \sum_{(i,j) \in E} \mathbb{I}\{z(i) = k, z(j) = l\}$ , which means that the edges  $\{(i,j)\}_{z(i)=k, z(j)=l}$  in the base graph  $G = (V, E)$  are contracted as a new edge  $(k, l)$  in  $\tilde{G} = (\tilde{V}, \tilde{E})$  with  $\omega_{kl}$  as the weight.

**Proposition 3.1.** *Suppose  $G = (V, E)$  is connected and  $\mathbf{1}_p^T w \neq 0$ . Then for any  $\gamma \in \{0, 1\}^m$ , (22) is a well-defined density function on the  $(s-1)$ -dimensional subspace  $\{\tilde{\theta} \in \mathbb{R}^s : w^T Z_\gamma \tilde{\theta} = 0\}$ . Moreover, for an arbitrary design matrix  $X \in \mathbb{R}^{n \times p}$ , the distribution of  $\theta$  that follows (3) weakly converges to that of  $Z_\gamma \tilde{\theta}$  as  $v_0 \rightarrow 0$ .*

Motivated by Proposition 3.1, a limiting version of (7) for  $v_0 = 0$  is defined as follows,

$$y|\alpha, \tilde{\theta}, \gamma, \sigma^2 \sim N(X(\alpha w + Z_\gamma \tilde{\theta}), \sigma^2 I_n). \quad (24)$$

Then,  $p(\tilde{\theta}|\gamma, \sigma^2)$  is given by (22), and  $p(\alpha|\sigma^2)$ ,  $p(\gamma|\eta)$ ,  $p(\eta)$ ,  $p(\sigma^2)$  are specified in (2) and (4)-(6). The posterior distribution of  $\gamma$  has the formula

$$\begin{aligned} p(\gamma|y) &\propto \int \int \int \int p(y, \alpha, \tilde{\theta}, \gamma, \eta, \sigma^2) d\alpha d\tilde{\theta} d\eta d\sigma^2 \\ &= \int p(\sigma^2) \int p(\alpha|\sigma^2) \int p(y|\alpha, \tilde{\theta}, \gamma, \sigma^2) p(\tilde{\theta}|\gamma, \sigma^2) d\tilde{\theta} d\alpha d\sigma^2 \int p(\gamma|\eta) p(\eta) d\eta. \end{aligned}$$

A standard calculation using conjugacy gives

$$\begin{aligned} p(\gamma|y) &\propto \left( \frac{\det_{Z_\gamma^T w}(Z_\gamma^T \tilde{L}_\gamma Z_\gamma)}{\det_{Z_\gamma^T w}(Z_\gamma^T (X^T X + \tilde{L}_\gamma) Z_\gamma)} \right)^{1/2} \left( \frac{\nu}{\nu + w^T X^T (I_n - R_\gamma) X w} \right)^{1/2} \\ &\quad \times \left( y^T (I_n - R_\gamma) y - \frac{|w^T X^T (I_n - R_\gamma) y|^2}{\nu + w^T X^T (I_n - R_\gamma) X w} + b \right)^{-\frac{n+a}{2}} \\ &\quad \times \frac{\text{Beta}\left(\sum_{(i,j) \in E} \gamma_{ij} + A - 1, \sum_{(i,j) \in E} (1 - \gamma_{ij}) + B - 1\right)}{\text{Beta}(A, B)}, \end{aligned} \quad (25)$$

where

$$R_\gamma = X Z_\gamma (Z_\gamma^T (X^T X + \tilde{L}_\gamma) Z_\gamma)^{-1} Z_\gamma^T X^T.$$

This defines the model selection score  $g(\gamma) = \log p(\gamma|y)$  up to a universal additive constant. The Bayesian model selection procedure evaluates  $g(\gamma)$  on the solution path  $\{\hat{\gamma}(v_0)\}_{0 < v_0 \leq v_1}$  and selects the best model with the highest value of  $g(\gamma)$ .

## 4 Clustering: A New Deal

### 4.1 A Multivariate Extension

Before introducing our new Bayesian clustering model, we need a multivariate extension of the general framework (7) to model a matrix observation  $y \in \mathbb{R}^{n \times d}$ . With a design matrix  $X \in \mathbb{R}^{n \times p}$ , the dimension of  $\theta$  is now  $p \times d$ . We denote the  $i$ th row of  $\theta$  by  $\theta_i$ . With the grounding vector  $w \in \mathbb{R}^p$ , the distribution  $p(y|\alpha, \theta, \sigma^2)p(\alpha|\sigma^2)p(\theta|\gamma, \sigma^2)$  is given by

$$y|\alpha, \theta, \sigma^2 \sim N(X(w\alpha^T + \theta), \sigma^2 I_n \otimes I_d), \quad (26)$$

$$\alpha|\sigma^2 \sim N\left(0, \frac{\sigma^2}{\nu} I_d\right), \quad (27)$$

$$\theta|\gamma, \sigma^2 \sim p(\theta|\gamma, \sigma^2) \propto \prod_{(i,j) \in E} \exp\left(-\frac{\|\theta_i - \theta_j\|^2}{2\sigma^2[v_0\gamma_{ij} + v_1(1 - \gamma_{ij})]}\right) \mathbb{I}\{\theta \in \Theta_w\}, \quad (28)$$

where  $\Theta_w = \{\theta \in \mathbb{R}^{p \times d} : w^T \theta = 0\}$ . The prior distributions on  $\gamma, \eta, \sigma^2$  are the same as (4)-(6). Moreover, the multivariate spike-and-slab Laplacian prior (28) is supported on a  $d(p-1)$ -dimensional subspace  $\Theta_w$ , and is well-defined as long as  $\mathbb{1}_p^T w \neq 0$  for the same reason stated in Proposition 2.1.

The multivariate extension can be understood as the task of learning  $d$  individual graphs for each column of  $\theta$ . Instead of modeling the  $d$  graph separately by  $\gamma^{(1)}, \dots, \gamma^{(d)}$  using (7), we assume the  $d$  columns of  $\theta$  share the same structure by imposing the condition  $\gamma^{(1)} = \dots = \gamma^{(d)}$ .

An immediate example is a Bayesian multitask learning problem with group sparsity. It can be viewed as a multivariate extension of Example 2.1. With the same argument in Example 2.1, (26)-(28) is specialized to

$$\begin{aligned} y|\theta, \sigma^2 &\sim N(X\theta, \sigma^2 I_n \otimes I_d), \\ \theta|\gamma, \sigma^2 &\sim p(\theta|\gamma, \sigma^2) \propto \prod_{i=1}^p \exp\left(-\frac{\|\theta_i\|^2}{2\sigma^2[v_0\gamma_i + v_1(1 - \gamma_i)]}\right). \end{aligned}$$

To close this subsection, let us mention that the model (26)-(28) can be easily modified to accommodate a heteroscedastic setting. For example, one can replace the  $\sigma^2 I_n \otimes I_d$  in (26) by a more general  $I_n \otimes \text{diag}(\sigma_1^2, \dots, \sigma_d^2)$ , and then make corresponding changes to (27) and (28) as well.

### 4.2 Model Description

Consider the likelihood

$$y|\alpha, \theta, \sigma^2 \sim N(\mathbb{1}_n \alpha^T + \theta, \sigma^2 I_n \otimes I_d), \quad (29)$$

with the prior distribution of  $\alpha|\sigma^2$  specified by (27). The clustering model uses the following form of (28),

$$p(\theta, \mu|\gamma, \sigma^2) \propto \prod_{i=1}^n \prod_{j=1}^k \exp\left(-\frac{\|\theta_i - \mu_j\|^2}{2\sigma^2[v_0\gamma_{ij} + v_1(1 - \gamma_{ij})]}\right) \mathbb{I}\{\mathbb{1}_n^T \theta = 0\}. \quad (30)$$

Here, both vectors  $\theta_i$  and  $\mu_j$  are in  $\mathbb{R}^d$ . The prior distribution (30) can be derived from (28) by replacing  $\theta$  in (28) with  $(\theta, \mu)$  and specifying the base graph as a complete bipartite graph between  $\theta$  and  $\mu$ . We impose the restriction that

$$\sum_{j=1}^k \gamma_{ij} = 1, \quad (31)$$

for all  $i \in [n]$ . Then,  $\mu_1, \dots, \mu_k$  are latent variables that can be interpreted as the clustering centers, and each  $\theta_i$  is connected to one of the clustering centers.

To fully specify the clustering model, the prior distribution of  $\gamma$  is given by (4) with  $\Gamma$  being the set of all  $\{\gamma_{ij}\}$  that satisfies (31). Equivalently,

$$(\gamma_{i1}, \dots, \gamma_{ik}) \sim \text{Uniform}(\{e_j\}_{j=1}^k), \quad (32)$$

independently for all  $i \in [n]$ , where  $e_j$  is a vector with 1 on the  $j$ th entry and 0 elsewhere. Finally, the prior of  $\sigma^2$  is given by (6).

### 4.3 EM Algorithm

The EM algorithm can be derived by following the idea developed in Section 3.2. In the current setting, the lower bound (18) becomes

$$\begin{aligned} & \log \sum_{T \in \text{spt}(K_{n,k})} \prod_{i=1}^n \prod_{j=1}^k [v_0^{-1} \gamma_{ij} + v_1^{-1} (1 - \gamma_{ij})] \\ & \geq \sum_{i=1}^n \sum_{j=1}^k r_{ij} \log [v_0^{-1} \gamma_{ij} + v_1^{-1} (1 - \gamma_{ij})] + \log |\text{spt}(K_{n,k})|, \end{aligned} \quad (33)$$

where  $K_{n,k}$  is the complete bipartite graph. By symmetry, the effective resistance  $r_{ij} = r$  is a constant independent of  $(i, j)$ . Thus, (33) can be written as

$$\begin{aligned} & r \sum_{i=1}^n \sum_{j=1}^k \log [v_0^{-1} \gamma_{ij} + v_1^{-1} (1 - \gamma_{ij})] + \log |\text{spt}(K_{n,k})| \\ & = r \log(v_0^{-1}) \sum_{i=1}^n \sum_{j=1}^k \gamma_{ij} + r \log(v_1^{-1}) \sum_{i=1}^n \sum_{j=1}^k (1 - \gamma_{ij}) + \log |\text{spt}(K_{n,k})| \\ & = rn \log(v_0^{-1}) + rn(k-1) \log(v_1^{-1}) + \log |\text{spt}(K_{n,k})|, \end{aligned} \quad (34)$$

where the last equality is derived from (31). Therefore, for the clustering model, the lower bound (18) is a constant independent of  $\{\gamma_{ij}\}$ . As a result, the lower bound of the objective function of the EM algorithm becomes

$$\sum_{\gamma} q(\gamma) \log \frac{p(y|\alpha, \theta, \sigma^2) p(\alpha|\sigma^2) \tilde{p}(\theta, \mu|\gamma, \sigma^2) p(\gamma) p(\sigma^2)}{q(\gamma)}, \quad (36)$$

with

$$\tilde{p}(\theta, \mu | \gamma, \sigma^2) = \text{const} \times \frac{1}{(2\pi\sigma^2)^{(n+k-1)d/2}} \prod_{i=1}^n \prod_{j=1}^k \exp\left(-\frac{\|\theta_i - \mu_j\|^2}{2\sigma^2[v_0\gamma_{ij} + v_1(1 - \gamma_{ij})]}\right),$$

and the algorithm is to maximize (36) over  $q, \alpha, \theta \in \{\theta : \mathbf{1}_n^T \theta = 0\}$  and  $\sigma^2$ .

Maximizing (36) over  $q$ , we obtain the E-step as

$$q_{ij}^{\text{new}} = \frac{\exp\left(-\frac{\|\theta_i - \mu_j\|^2}{2\sigma^2 \bar{v}}\right)}{\sum_{l=1}^k \exp\left(-\frac{\|\theta_i - \mu_l\|^2}{2\sigma^2 \bar{v}}\right)}, \quad (37)$$

independently for all  $i \in [n]$ , where  $\bar{v}^{-1} = v_0^{-1} - v_1^{-1}$ , and we have used the notation

$$q_{ij} = q((\gamma_{i1}, \dots, \gamma_{ik}) = e_j).$$

It is interesting to note that the E-step only depends on  $v_0$  and  $v_1$  through  $\bar{v}$ . Maximizing (36) over  $\alpha, \theta \in \{\theta : \mathbf{1}_n^T \theta = 0\}, \mu, \sigma^2$ , we obtain the M-step as

$$\begin{aligned} (\alpha^{\text{new}}, \theta^{\text{new}}, \mu^{\text{new}}) &= \underset{\alpha, \mathbf{1}_n^T \theta = 0, \mu}{\text{argmin}} F(\alpha, \theta, \mu; q^{\text{new}}), \\ (\sigma^2)^{\text{new}} &= \frac{F(\alpha^{\text{new}}, \theta^{\text{new}}, \mu^{\text{new}}; q^{\text{new}}) + b}{(2n + k)d + a + 2}, \end{aligned} \quad (38)$$

where

$$F(\alpha, \theta, \mu; q) = \|y - \mathbf{1}_n \alpha^T - \theta\|_F^2 + \nu \|\alpha\|^2 + \sum_{i=1}^n \sum_{j=1}^k \left( \frac{q_{ij}}{v_0} + \frac{1 - q_{ij}}{v_1} \right) \|\theta_i - \mu_j\|^2.$$

Note that for all  $\theta$  such that  $\mathbf{1}_n^T \theta = 0$ , we have

$$\|y - \mathbf{1}_n \alpha^T - \theta\|_F^2 = \|n^{-1} \mathbf{1}_n \mathbf{1}_n^T y - \mathbf{1}_n \alpha^T\|_F^2 + \|y - n^{-1} \mathbf{1}_n \mathbf{1}_n^T y - \theta\|_F^2,$$

and thus the M-step (38) can be solved separately for  $\alpha$  and  $(\theta, \mu)$ .

#### 4.4 A Connection to Bipartite Graph Projection

The clustering model (30) involves latent variables  $\mu$  that do not appear in the likelihood (29). This allows us to derive an efficient EM algorithm in Section 4.3. To better understand (30), we connect the bipartite graphical structure between  $\theta$  and  $\mu$  to a graphical structure on  $\theta$  alone. Given a  $\gamma = \{\gamma_{ij}\}$  that satisfies (31), we call it non-degenerate if  $\sum_{i=1}^n \gamma_{ij} > 0$  for all  $j \in [k]$ . In other words, none of the  $k$  clusters is empty.

**Proposition 4.1.** *Let the conditional distribution of  $\theta, \mu | \gamma, \sigma^2$  be specified by (30) with some non-degenerate  $\gamma$ . Then, the distribution of  $\theta | \gamma, \sigma^2$  weakly converges to*

$$p(\theta | \gamma, \sigma^2) \propto \prod_{1 \leq i < l \leq n} \exp\left(-\frac{\lambda_{il} \|\theta_i - \theta_l\|^2}{2\sigma^2 v_0}\right) \mathbb{I}\{\mathbf{1}_n^T \theta = 0\}, \quad (39)$$

as  $v_1 \rightarrow \infty$ , where  $\lambda_{il} = \sum_{j=1}^k \gamma_{ij} \gamma_{lj} / n_j$  with  $n_j = \sum_{i=1}^n \gamma_{ij}$  being the size of the  $j$ th cluster.

The formula (39) resembles (3), except that  $\lambda$  encodes a clustering structure. By the definition of  $\lambda_{il}$ , if  $\theta_i$  and  $\theta_l$  are in different clusters,  $\lambda_{il} = 0$ , and otherwise,  $\lambda_{il}$  takes the inverse of the size of the cluster that both  $\theta_i$  and  $\theta_l$  belong to. The relation between (30) and (39) can be understood from the operations of graph projection and graph lift, in the sense that the weighted graph  $\lambda$ , with nodes  $\theta$ , is a projection of  $\gamma$ , a bipartite graph between nodes  $\theta$  and nodes  $\mu$ . Conversely,  $\gamma$  is said to be a graph lift of  $\lambda$ . Observe that the clustering structure of (39) is combinatorial, and therefore it is much easier to work with the bipartite structure in (30) with latent variables.

## 4.5 A Connection to Gaussian Mixture Models

We establish a connection to Gaussian mixture models. We first give the following result.

**Proposition 4.2.** *Let the conditional distribution of  $\theta, \mu | \gamma, \sigma^2$  be specified by (30). Then, as  $v_0 \rightarrow 0$ , this conditional distribution weakly converges to the distribution specified by the following sampling process:  $\theta = \gamma\mu$  and  $\mu | \gamma, \sigma^2$  is sampled from*

$$p(\mu | \gamma, \sigma^2) \propto \prod_{1 \leq j < l \leq k} \exp \left( -\frac{(n_j + n_l) \|\mu_j - \mu_l\|^2}{2\sigma^2 v_1} \right) \mathbb{I}\{\mathbf{1}_n^T \gamma \mu = 0\}, \quad (40)$$

where  $n_j = \sum_{i=1}^n \gamma_{ij}$  being the size of the  $j$ th cluster.

With this proposition, we can see that as  $v_0 \rightarrow 0$ , the clustering model specified by (29), (27) and (30) becomes

$$y | \alpha, \mu, \gamma, \sigma^2 \sim N(\mathbf{1}_n \alpha^T + \gamma \mu, \sigma^2 I_n \otimes I_d), \quad (41)$$

with  $\alpha | \sigma^2$  distributed by (27) and  $\mu | \gamma, \sigma^2$  distributed by (40). The likelihood function (41) is commonly used in Gaussian mixture models, which encodes an exact clustering structure. Therefore, with a finite  $v_0$ , the model specified by (29), (27) and (30) can be interpreted as a relaxed version of the Gaussian mixture models that leads to an approximate clustering structure.

## 4.6 Adaptation to the Number of Clusters

The number  $k$  in (30) should be understood as an upper bound of the number of clusters. Even though the EM algorithm outputs  $k$  cluster centers  $\{\hat{\mu}_1, \dots, \hat{\mu}_k\}$ , these  $k$  cluster centers will be automatically grouped according to their own closeness as we vary the value of  $v_0$ . Generally speaking, for a very small  $v_0$  (the Gaussian mixture model in Section 4.5, for example),  $\{\hat{\mu}_1, \dots, \hat{\mu}_k\}$  will take  $k$  vectors that are not close to each other. As we increase  $v_0$ , the clustering centers  $\{\hat{\mu}_1, \dots, \hat{\mu}_k\}$  start to merge, and eventually for a sufficiently large  $v_0$ , they will all converge to a single vector. In short,  $v_0$  parametrizes the solution path of our clustering algorithm, and on this solution path, the *effective* number of clusters increases as the value of  $v_0$  increases.

We illustrate this point by a simple numerical example. Consider the observation  $y = (4, 2, -2, 4)^T \in \mathbb{R}^{4 \times 1}$ . We fit our clustering model with  $k \in \{2, 3, 4\}$ . Figure 1 visualizes the output of the EM algorithm  $(\hat{\mu}, \hat{\theta})$  as  $v_0$  varies. It is clear that the solution path always starts at  $\{\hat{\mu}_1, \dots, \hat{\mu}_k\}$  of different values. Then, as  $v_0$  increases, the solution path has various phase transitions where the closest two  $\hat{\mu}_j$ 's merge. In the end, for a sufficiently large  $v_0$ , the clustering centers  $\{\hat{\mu}_1, \dots, \hat{\mu}_k\}$  all merge to a common value.

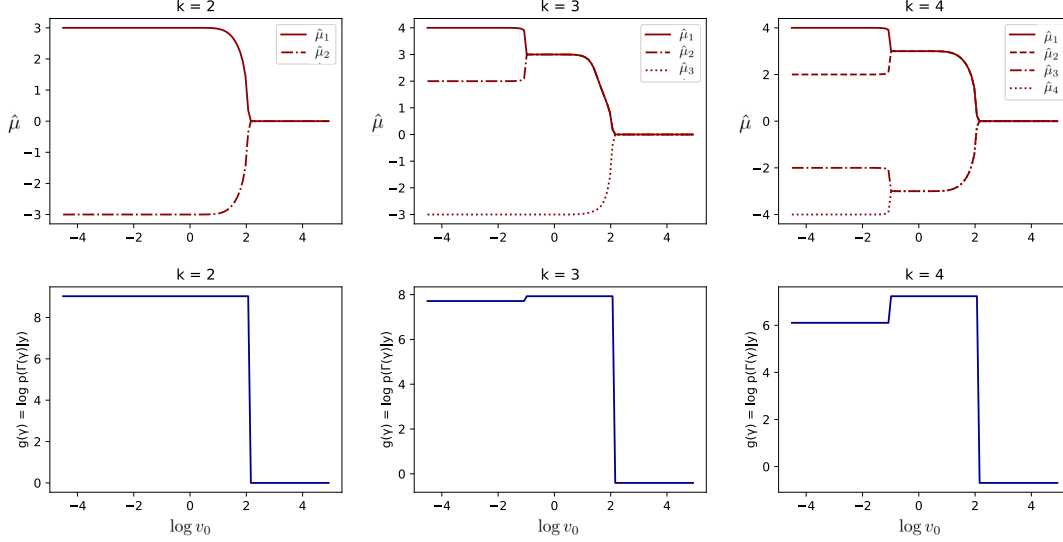


Figure 1: (Top) Solution paths of  $\hat{\mu}$  with different choices of  $k$ ; (Bottom) Model selection scores on the solution paths.

To explain this phenomenon, it is most clear to investigate the case  $k = 2$ . Then, the M-step (38) updates  $\mu$  according to

$$\begin{aligned}\mu_1^{\text{new}} &= \underset{\mu_1}{\operatorname{argmin}} \sum_{i=1}^n \left( \frac{q_{i1}}{v_0} + \frac{1 - q_{i1}}{v_1} \right) \|\theta_i - \mu_1\|^2 \\ \mu_1^{\text{new}} &= \underset{\mu_2}{\operatorname{argmin}} \sum_{i=1}^n \left( \frac{q_{i2}}{v_0} + \frac{1 - q_{i2}}{v_1} \right) \|\theta_i - \mu_2\|^2.\end{aligned}$$

Observe that both  $\mu_1^{\text{new}}$  and  $\mu_2^{\text{new}}$  are weighted averages of  $\{\theta_1, \dots, \theta_n\}$ , and the only difference between  $\mu_1^{\text{new}}$  and  $\mu_2^{\text{new}}$  lies in the weights. According to the E-step (37),

$$\begin{aligned}q_{i1} &= \frac{\exp\left(-\frac{\|\theta_i - \mu_1\|^2}{2\sigma^2\bar{v}}\right)}{\exp\left(-\frac{\|\theta_i - \mu_1\|^2}{2\sigma^2\bar{v}}\right) + \exp\left(-\frac{\|\theta_i - \mu_2\|^2}{2\sigma^2\bar{v}}\right)} \\ q_{i2} &= \frac{\exp\left(-\frac{\|\theta_i - \mu_2\|^2}{2\sigma^2\bar{v}}\right)}{\exp\left(-\frac{\|\theta_i - \mu_1\|^2}{2\sigma^2\bar{v}}\right) + \exp\left(-\frac{\|\theta_i - \mu_2\|^2}{2\sigma^2\bar{v}}\right)},\end{aligned}$$

and we recall that  $\bar{v}^{-1} = v_0^{-1} - v_1^{-1}$ . Therefore, as  $v_0 \rightarrow \infty$ ,  $q_{i1} \rightarrow 1/2$  and  $q_{i2} \rightarrow 1/2$ , which results in the phenomenon that  $\mu_1^{\text{new}}$  and  $\mu_2^{\text{new}}$  merge to the same value. The same reasoning also applies to  $k \geq 2$ .

## 4.7 Model Selection

In this section, we discuss how to select a clustering structure from the solution path of the EM algorithm. According to the discussion in Section 4.6, we should understand  $k$  as an upper bound of the number of clusters, and the estimator of the number of clusters will be part of the output of the model selection procedure. The general recipe of our method follows the framework discussed in Section 3.3, but some nontrivial twist is required in the clustering problem. To make the presentation clear, the model selection procedure will be introduced in two parts. We will first propose our model selection score, and then we will describe a method that extracts a clustering structure from the output of the EM algorithm.

**The model selection score.** For any  $\gamma \in \{0, 1\}^{n \times k}$  that satisfies (31), we can calculate the posterior probability  $p(\gamma|y)$  with  $v_0 = 0$ . This can be done by the connection to Gaussian mixture models discussed in Section 4.5. To be specific, the calculation follows the formula

$$p(\gamma|y) = \int \int \int p(y|\alpha, \mu, \gamma, \sigma^2) p(\alpha|\sigma^2) p(\mu|\gamma, \sigma^2) p(\sigma^2) p(\gamma) d\alpha d\mu d\sigma^2,$$

where  $p(y|\alpha, \mu, \gamma, \sigma^2)$ ,  $p(\alpha|\sigma^2)$ ,  $p(\mu|\gamma, \sigma^2)$ ,  $p(\sigma^2)$ , and  $p(\gamma)$  are specified by (29), (27), (40), (6) and (32). A standard calculation gives the formula

$$p(\gamma|y) \propto \left( \frac{\nu}{\nu + n} \times \frac{\det_{\gamma^T \mathbb{1}_n}(\bar{L}_\gamma)}{\det_{\gamma^T \mathbb{1}_n}(\bar{L}_\gamma + \gamma^T \gamma)} \right)^{d/2} \times \left[ \frac{\nu n}{\nu + n} \|n^{-1} \mathbb{1}_n y\|^2 + \text{Tr} \left( (y - n^{-1} \mathbb{1}_n \mathbb{1}_n^T y)^T (I_n - \gamma(\bar{L}_\gamma + \gamma^T \gamma) \gamma^T) (y - n^{-1} \mathbb{1}_n \mathbb{1}_n^T y) \right) \right]^{-\frac{nd+a}{2}}, \quad (42)$$

where  $\bar{L}_\gamma = (\mathbb{1}_{k \times n} \gamma + \gamma^T \mathbb{1}_{n \times k} - 2\gamma^T \gamma)/v_1$  is the graph Laplacian of the weighted adjacency matrix, which satisfies

$$\text{Tr}(\mu^T \bar{L}_\gamma \mu) = \sum_{1 \leq j < l \leq k} \frac{n_j + n_l}{v_1} \|\mu_j - \mu_l\|^2.$$

Recall that  $n_j = \sum_{i=1}^n \gamma_{ij}$  is the size of the  $j$ th cluster.

However, the goal of the model selection is to select a clustering structure, and it is possible that different  $\gamma$ 's may correspond to the same clustering structure due to label permutation. To overcome this issue, we need to sum over all equivalent  $\gamma$ 's. Given a  $\gamma \in \{0, 1\}^{n \times k}$  that satisfies (31), define a symmetric membership matrix  $\Gamma(\gamma) \in \{0, 1\}^{n \times n}$  by

$$\Gamma_{il}(\gamma) = \mathbb{I} \left\{ \sum_{j=1}^k \gamma_{ij} \gamma_{lj} = 1 \right\}.$$

In other words,  $\Gamma_{il}(\gamma) = 1$  if and only if  $i$  and  $l$  are in the same cluster. It is easy to see that every clustering structure can be uniquely represented by a symmetric membership matrix. We define the posterior probability of a clustering structure  $\Gamma$  by

$$p(\Gamma|y) = \sum_{\gamma \in \{\gamma: \Gamma(\gamma) = \Gamma\}} p(\gamma|y).$$

The explicit calculation of the above summation is not necessary. A shortcut can be derived from the fact that  $p(\gamma|y) = p(\gamma'|y)$  if  $\Gamma(\gamma) = \Gamma(\gamma')$ . This immediately implies that  $p(\Gamma|y) = |\Gamma|p(\gamma|y)$  for any  $\gamma$  that satisfies  $\Gamma(\gamma) = \Gamma$ . Suppose  $\Gamma$  encodes a clustering structure with  $\tilde{k}$  nonempty clusters, and then we have  $|\Gamma| = \binom{k}{\tilde{k}}\tilde{k}!$ . This leads to the model selection score

$$g(\gamma) = \log p(\Gamma(\gamma)|y) = \log p(\gamma|y) + \log \left[ \binom{k}{\tilde{k}}\tilde{k}! \right], \quad (43)$$

for any  $\gamma \in \{0, 1\}^{n \times k}$  that satisfies (31), and  $\tilde{k}$  above is calculated by  $\tilde{k} = \sum_{j=1}^k \max_{1 \leq i \leq n} \gamma_{ij}$ , the effective number of clusters.

**Extraction of clustering structures from the EM algorithm.** Let  $\hat{\mu}$  and  $\hat{q}$  be outputs of the EM algorithm, and we discuss how to obtain  $\hat{\gamma}$  that encodes a meaningful clustering structure to be evaluated by the model selection score (43). It is very tempting to directly threshold  $\hat{q}$  as is done in Section 3.3. However, as has been discussed in Section 4.6, the solution paths of  $\{\mu_1, \dots, \mu_k\}$  merge at some values of  $v_0$ . Therefore, we should treat the clusters whose clustering centers merge together as a single cluster.

Given  $\hat{\mu}_1, \dots, \hat{\mu}_k$  output by the M-step, we first merge  $\hat{\mu}_j$  and  $\hat{\mu}_l$  whenever  $\|\hat{\mu}_j - \hat{\mu}_l\| \leq \epsilon$ . The number  $\epsilon$  is taken as  $10^{-8}$ , the square root of the machine precision, in our code. This forms a partition  $[k] = \cup_{l=1}^{\tilde{k}} \mathcal{G}_l$  for some  $\tilde{k} \leq k$ . Then, by taking average within each group, we obtain a reduced collection of clustering centers  $\tilde{\mu}_1, \dots, \tilde{\mu}_{\tilde{k}}$ . In other words,  $\tilde{\mu}_l = |\mathcal{G}_l|^{-1} \sum_{j \in \mathcal{G}_l} \hat{\mu}_j$ .

The  $\hat{q} \in [0, 1]^{n \times k}$  output by the E-step should also be reduced to  $\tilde{q} \in [0, 1]^{n \times \tilde{k}}$  as well. Note that  $\hat{q}_{ij}$  is the estimated posterior probability that the  $i$ th node belongs to the  $j$ th cluster. This means that  $\tilde{q}_{il}$  is the estimated posterior probability that the  $i$ th node belongs to the  $l$ th reduced cluster. An explicit formula is given by  $\tilde{q}_{il} = \sum_{j \in \mathcal{G}_l} \hat{q}_{ij}$ .

With the reduced posterior probability  $\tilde{q}$ , we simply apply thresholding to obtain  $\hat{\gamma}$ . We have  $(\hat{\gamma}_{i1}, \dots, \hat{\gamma}_{ik}) = e_j$  if  $j = \arg\max_{1 \leq l \leq \tilde{k}} \tilde{q}_{il}$ . Recall that  $e_j$  is a vector with 1 on the  $j$ th entry and 0 elsewhere. Note that according to this construction, we always have  $\hat{\gamma}_{ij} = 0$  whenever  $j > \tilde{k}$ . This does not matter, because the model selection score (43) does not depend on the clustering labels. Finally, the  $\hat{\gamma}$  constructed according to the above procedure will be evaluated by  $g(\hat{\gamma})$  defined by (43).

In the toy example with four data points  $y = (4, 2, -2, 4)^T$ , the model selection score is computed along the solution path. According to Figure 1, the model selection procedure suggests that a clustering structure with two clusters  $\{4, 2\}$  and  $\{-2, -4\}$  is the most plausible one. We also note that the curve of  $g(\gamma)$  has sharp phase transitions whenever the solution paths  $\mu$  merge.

## 5 Extensions with Graph Algebra

In many applications, it is useful to have a model that imposes both row and column structures on a high-dimensional matrix  $\theta \in \mathbb{R}^{p_1 \times p_2}$ . We list some important examples below.

1. *Biclustering*. In applications such as gene expression data analysis, one needs to cluster both samples and features. This task imposes a clustering structure for both rows and columns of the data matrix [24, 7].
2. *Block sparsity*. In problems such as planted clique detection [14] and submatrix localization [22], the matrix can be viewed as the sum of a noise background plus a submatrix of signals with unknown locations. Equivalently, it can be modeled by simultaneous row and column sparsity [32].
3. *Sparse clustering*. Suppose the data matrix exhibits a clustering structure for its rows and a sparsity structure for its columns, then we have a sparse clustering problem [50]. For this task, we need to select nonzero column features in order to accurately cluster the rows.

For the problems listed above, the row and column structures can be modeled by graphs  $\gamma_1$  and  $\gamma_2$ . Then, the structure of the matrix  $\theta$  is induced by a notion of graph product of  $\gamma_1$  and  $\gamma_2$ . In this section, we introduce tools from graph algebra including Cartesian product and Kronecker product to build complex structure from simple components.

We first introduce the likelihood of the problem. To cope with many useful models, we assume that the observation can be organized as a matrix  $y \in \mathbb{R}^{n_1 \times n_2}$ . Then, the specific setting of a certain problem can be encoded by design matrices  $X_1 \in \mathbb{R}^{n_1 \times p_1}$  and  $X_2 \in \mathbb{R}^{n_2 \times p_2}$ . The likelihood is defined by

$$y|\alpha, \theta, \sigma^2 \sim N(X_1(\alpha w + \theta)X_2^T, \sigma^2 I_{n_1} \otimes I_{n_2}). \quad (44)$$

The matrix  $w \in \mathbb{R}^{p_1 \times p_2}$  is assumed to have rank one, and can be decomposed as  $w = w_1 w_2^T$  for some  $w_1 \in \mathbb{R}^{p_1}$  and  $w_2 \in \mathbb{R}^{p_2}$ . The prior distribution of the scalar is simply given by

$$\alpha|\sigma^2 \sim N(0, \sigma^2/\nu). \quad (45)$$

We then need to build prior distributions of  $\theta$  that is supported on  $\Theta_w = \{\theta \in \mathbb{R}^{p_1 \times p_2} : \text{Tr}(w\theta^T) = 0\}$  using Cartesian and Kronecker products.

### 5.1 Cartesian Product

We start with the definition of the Cartesian product of two graphs.

**Definition 5.1.** *Given two graphs  $G_1 = (V_1, E_1)$  and  $G_2 = (V_2, E_2)$ , their Cartesian product  $G = G_1 \square G_2$  is defined with the vertex set  $V_1 \times V_2$ . Its edge set contains  $((x_1, x_2), (y_1, y_2))$  if and only if  $x_1 = y_1$  and  $(x_2, y_2) \in E_2$  or  $(x_1, y_1) \in E_1$  and  $x_2 = y_2$ .*

According to the definition, it can be checked that for two graphs of sizes  $p_1$  and  $p_2$ , the adjacency matrix, the Laplacian and the incidence matrix of the Cartesian product enjoy the relations

$$\begin{aligned} A_{1\Box 2} &= A_2 \otimes I_{p_1} + I_{p_2} \otimes A_1, \\ L_{1\Box 2} &= L_2 \otimes I_{p_1} + I_{p_2} \otimes L_1, \\ D_{1\Box 2} &= [D_2 \otimes I_{p_1}; I_{p_2} \otimes D_1]. \end{aligned}$$

Given graphs  $\gamma_1$  and  $\gamma_2$  that encode row and column structures of  $\theta$ , we introduce the following prior distribution

$$\begin{aligned} p(\theta|\gamma_1, \gamma_2, \sigma^2) &\propto \prod_{(i,j) \in E_1} \exp\left(-\frac{\|\theta_{i*} - \theta_{j*}\|^2}{2\sigma^2[v_0\gamma_{1,ij} + v_1(1 - \gamma_{1,ij})]}\right) \\ &\times \prod_{(k,l) \in E_2} \exp\left(-\frac{\|\theta_{*k} - \theta_{*l}\|^2}{2\sigma^2[v_0\gamma_{2,kl} + v_1(1 - \gamma_{2,kl})]}\right) \mathbb{I}\{\theta \in \Theta_w\}. \end{aligned} \quad (46)$$

Here,  $E_1$  and  $E_2$  are the base graphs of the row and column structures. According to its form, the prior distribution (46) models both pairwise relations of rows and those of columns based on  $\gamma_1$  and  $\gamma_2$ , respectively. To better understand (46), we can write it in the following equivalent form,

$$p(\theta|\gamma_1, \gamma_2, \sigma^2) \propto \exp\left(-\frac{1}{2\sigma^2} \text{vec}(\theta)^T (L_{\gamma_2} \otimes I_{p_1} + I_{p_2} \otimes L_{\gamma_1}) \text{vec}(\theta)\right) \mathbb{I}\{\theta \in \Theta_w\}, \quad (47)$$

where  $L_{\gamma_1} \in \mathbb{R}^{p_1 \times p_1}$  and  $L_{\gamma_2} \in \mathbb{R}^{p_2 \times p_2}$  are Laplacian matrices of the weighted graphs  $\{v_0\gamma_{1,ij} + v_1(1 - \gamma_{1,ij})\}$  and  $\{v_0\gamma_{2,kl} + v_1(1 - \gamma_{2,kl})\}$ , respectively. Therefore, by Definition 5.1,  $p(\theta|\gamma_1, \gamma_2, \sigma^2)$  is a spike-and-slab Laplacian prior  $p(\theta|\gamma, \sigma^2)$  defined in (3) with  $\gamma = \gamma_1 \Box \gamma_2$ , and the well-definedness is guaranteed by Proposition 2.1.

To complete the Bayesian model, the distribution of  $(\gamma_1, \gamma_2, \sigma^2)$  are specified by

$$\gamma_1, \gamma_2 | \eta_1, \eta_2 \sim \prod_{(i,j) \in E_1} \eta_1^{\gamma_{1,ij}} (1 - \eta_1)^{1 - \gamma_{1,ij}} \prod_{(i,j) \in E_2} \eta_2^{\gamma_{2,kl}} (1 - \eta_2)^{1 - \gamma_{2,kl}}, \quad (48)$$

$$\eta_1, \eta_2 \sim \text{Beta}(A_1, B_1) \otimes \text{Beta}(A_2, B_2), \quad (49)$$

$$\sigma^2 \sim \text{InvGamma}(a/2, b/2). \quad (50)$$

We remark that it is possible to constrain  $\gamma_1$  and  $\gamma_2$  in some subsets  $\Gamma_1$  and  $\Gamma_2$  like (4). This extra twist is useful for a biclustering model that will be discussed in Section 5.3.

Note that in general the base graph  $G = G_1 \Box G_2$  is not a tree, and the derivation of the EM algorithm follows a similar argument in Section 3.2. Using the same argument in (18), we lower bound  $\log \sum_{T \in \text{spt}(G)} \sum_{e \in T} [v_0^{-1} \gamma_e + v_1^{-1} (1 - \gamma_e)]$  by

$$\sum_{e \in E_1 \Box E_2} r_e \log[v_0^{-1} \gamma_e + v_1^{-1} (1 - \gamma_e)] + \log |\text{spt}(G)|. \quad (51)$$

Since

$$E_1 \square E_2 = \{((i, k), (j, k)) : (i, j) \in E_1, k \in V_2\} \cup \{((i, k), (i, l)) : i \in V_1, (k, l) \in E_2\},$$

and  $\gamma = \gamma_1 \square \gamma_2$ , we can write (51) as

$$\begin{aligned} & \sum_{(i,j) \in E_1} \sum_{k=1}^{p_2} r_{(i,k),(j,k)} \log[v_0^{-1} \gamma_{1,ij} + v_1^{-1} (1 - \gamma_{1,ij})] \\ & + \sum_{(k,l) \in E_2} \sum_{i=1}^{p_1} r_{(i,k),(i,l)} \log[v_0^{-1} \gamma_{2,kl} + v_1^{-1} (1 - \gamma_{2,kl})] \\ = & \sum_{(i,j) \in E_1} r_{1,ij} \log[v_0^{-1} \gamma_{1,ij} + v_1^{-1} (1 - \gamma_{1,ij})] + \sum_{(k,l) \in E_2} r_{2,kl} \log[v_0^{-1} \gamma_{2,kl} + v_1^{-1} (1 - \gamma_{2,kl})], \end{aligned}$$

where

$$r_{1,ij} = \sum_{k=1}^{p_2} r_{(i,k),(j,k)} = \frac{1}{|\text{spt}(G)|} \sum_{k=1}^{p_2} \sum_{T \in \text{spt}(G)} \mathbb{I}\{((i, k), (j, k)) \in T\},$$

and  $r_{2,kl}$  is similarly defined.

Using the lower bound derived above, it is direct to derive the an EM algorithm, which consists of the following iterations,

$$q_{1,ij}^{\text{new}} = \frac{\eta_1 v_0^{-\frac{r_{1,ij}}{2}} e^{-\frac{1}{2\sigma^2 v_0} \|\theta_{i*} - \theta_{j*}\|^2}}{\eta_1 v_0^{-\frac{r_{1,ij}}{2}} e^{-\frac{1}{2\sigma^2 v_0} \|\theta_{i*} - \theta_{j*}\|^2} + (1 - \eta_1) v_1^{-\frac{r_{1,ij}}{2}} e^{-\frac{1}{2\sigma^2 v_1} \|\theta_{i*} - \theta_{j*}\|^2}}, \quad (52)$$

$$q_{2,kl}^{\text{new}} = \frac{\eta_2 v_0^{-\frac{r_{2,kl}}{2}} e^{-\frac{1}{2\sigma^2 v_0} \|\theta_{*k} - \theta_{*l}\|^2}}{\eta_2 v_0^{-\frac{r_{2,kl}}{2}} e^{-\frac{1}{2\sigma^2 v_0} \|\theta_{*k} - \theta_{*l}\|^2} + (1 - \eta_2) v_1^{-\frac{r_{2,kl}}{2}} e^{-\frac{1}{2\sigma^2 v_1} \|\theta_{*k} - \theta_{*l}\|^2}}, \quad (53)$$

$$(\alpha^{\text{new}}, \theta^{\text{new}}) = \underset{\alpha, \theta \in \Theta_w}{\text{argmin}} F(\alpha, \theta; q_1^{\text{new}}, q_2^{\text{new}}), \quad (54)$$

$$\begin{aligned} (\sigma^2)^{\text{new}} &= \frac{F(\alpha^{\text{new}}, \theta^{\text{new}}; q_1^{\text{new}}, q_2^{\text{new}}) + b}{n_1 n_2 + p_1 p_2 + a + 2}, \\ \eta_1^{\text{new}} &= \frac{A_1 - 1 + \sum_{(i,j) \in E_1} q_{1,ij}^{\text{new}}}{A_1 + B_1 - 2 + m_1}, \\ \eta_2^{\text{new}} &= \frac{A_2 - 1 + \sum_{(k,l) \in E_2} q_{2,kl}^{\text{new}}}{A_2 + B_2 - 2 + m_2}. \end{aligned} \quad (55)$$

The definition of the function  $F(\alpha, \theta; q_1, q_2)$  is given by

$$F(\alpha, \theta; q_1, q_2) = \|y - X_1(\alpha w + \theta) X_2^T\|_F^2 + \nu \alpha^2 + \text{vec}(\theta)^T (L_{q_2} \otimes I_{p_1} + I_{p_2} \otimes L_{q_1}) \text{vec}(\theta)$$

Though the E-steps (52) and (53) are straightforward, the M-step (54) is a quadratic programming of dimension  $p_1 p_2$ , which may become the computational bottleneck of the EM algorithm when the size of the problem is large. We will introduce a Dykstra-like algorithm to solve (54) in Appendix E.

## 5.2 Kronecker Product

The Kronecker product of two graphs is defined below.

**Definition 5.2.** *Given two graphs  $G_1 = (V_1, E_1)$  and  $G_2 = (V_2, E_2)$ , their Kronecker product  $G = G_1 \otimes G_2$  is defined with the vertex set  $V_1 \times V_2$ . Its edge set contains  $((x_1, x_2), (y_1, y_2))$  if and only if  $(x_1, y_1) \in E_1$  and  $(x_2, y_2) \in E_2$ .*

It is not hard to see that the adjacency matrix of two graphs has the formula  $A_{1 \otimes 2} = A_1 \otimes A_2$ , which gives the name of Definition 5.2. The prior distribution of  $\theta$  given row and column graphs  $\gamma_1$  and  $\gamma_2$  that we discuss in this subsection is

$$p(\theta|\gamma_1, \gamma_2, \sigma^2) \propto \prod_{(i,j) \in E_1} \prod_{(k,l) \in E_2} \exp \left( -\frac{(\theta_{ik} - \theta_{jl})^2}{2\sigma^2[v_0\gamma_{1,ij}\gamma_{2,kl} + v_1(1 - \gamma_{1,ij}\gamma_{2,kl})]} \right) \mathbb{I}\{\theta \in \Theta_w\}. \quad (56)$$

Again,  $E_1$  and  $E_2$  are the base graphs of the row and column structures. According to its form, the prior imposes a nearly block structure on  $\theta$  based on the graphs  $\gamma_1$  and  $\gamma_2$ . Moreover,  $p(\theta|\gamma_1, \gamma_2, \sigma^2)$  can be viewed as a spike-and-slab Laplacian prior  $p(\theta|\gamma, \sigma^2)$  defined in (3) with  $\gamma = \gamma_1 \otimes \gamma_2$ . The distribution of  $(\gamma_1, \gamma_2, \sigma^2)$  follows the same specification in (48)-(50).

To derive an EM algorithm, we follow the strategy in Section 3.2 and lower bound  $\log \sum_{T \in \text{spt}(G)} \sum_{e \in T} [v_0^{-1}\gamma_e + v_1^{-1}(1 - \gamma_e)]$  by

$$\sum_{(i,j) \in E_1} \sum_{(k,l) \in E_2} r_{(i,k),(j,l)} \log[v_0^{-1}\gamma_{1,ij}\gamma_{2,kl} + v_1^{-1}(1 - \gamma_{1,ij}\gamma_{2,kl})]. \quad (57)$$

Unlike the Cartesian product, the Kronecker product structure has a lower bound (57) that is not separable with respect to  $\gamma_1$  and  $\gamma_2$ . This makes the E-step combinatorial, and does not apply to a large-scale problem. To alleviate this computational barrier, we consider a variational EM algorithm that finds the best posterior distribution of  $\gamma_1, \gamma_2$  that can be factorized. In other words, instead of maximizing over all possible distribution  $q$ , we maximize over the mean-field class  $q \in \mathcal{Q}$ , with  $\mathcal{Q} = \{q(\gamma_1, \gamma_2) = q_1(\gamma_1)q_2(\gamma_2) : q_1, q_2\}$ . Then, the objective becomes

$$\max_{q_1, q_2} \max_{\alpha, \theta \in \Theta_2, \delta, \eta, \sigma^2} \sum_{\gamma_1, \gamma_2} q_1(\gamma_1)q_2(\gamma_2) \log \frac{\tilde{p}(y, \alpha, \theta, \delta, \gamma_1, \gamma_2, \eta, \sigma^2)}{q_1(\gamma_1)q_2(\gamma_2)},$$

where  $\tilde{p}(y, \alpha, \theta, \delta, \gamma_1, \gamma_2, \eta, \sigma^2)$  is obtained by replacing  $p(\theta|\gamma_1, \gamma_2, \sigma^2)$  with  $\tilde{p}(\theta|\gamma_1, \gamma_2, \sigma^2)$  in the joint distribution  $p(y, \alpha, \theta, \delta, \gamma_1, \gamma_2, \eta, \sigma^2)$ . Here,  $\log \tilde{p}(\theta|\gamma_1, \gamma_2, \sigma^2)$  is a lower bound for  $\log p(\theta|\gamma_1, \gamma_2, \sigma^2)$  with (57). The E-step of the variational EM is

$$\begin{aligned} q_1^{\text{new}}(\gamma_1) &\propto \exp \left( \sum_{\gamma_2} q_2(\gamma_2) \log \tilde{p}(y, \alpha, \theta, \delta, \gamma_1, \gamma_2, \eta, \sigma^2) \right), \\ q_2^{\text{new}}(\gamma_2) &\propto \exp \left( \sum_{\gamma_1} q_1^{\text{new}}(\gamma_1) \log \tilde{p}(y, \alpha, \theta, \delta, \gamma_1, \gamma_2, \eta, \sigma^2) \right). \end{aligned}$$

After some simplification, we have

$$q_{1,ij}^{\text{new}} = \frac{1}{(1-\eta_1) \prod_{(k,l) \in E_2} \left( v_1^{-\frac{r(i,k),(j,l)}{2}} e^{-\frac{1}{2\sigma^2 v_1} (\theta_{ik} - \theta_{jl})^2} \right)^{q_{2,kl}} + \frac{\eta_1 \prod_{(k,l) \in E_2} \left( v_0^{-\frac{r(i,k),(j,l)}{2}} e^{-\frac{1}{2\sigma^2 v_0} (\theta_{ik} - \theta_{jl})^2} \right)^{q_{2,kl}}}{1}}, \quad (58)$$

$$q_{2,kl}^{\text{new}} = \frac{1}{(1-\eta_2) \prod_{(i,j) \in E_1} \left( v_1^{-\frac{r(i,k),(j,l)}{2}} e^{-\frac{1}{2\sigma^2 v_1} (\theta_{ik} - \theta_{jl})^2} \right)^{q_{1,ij}^{\text{new}}} + \frac{\eta_2 \prod_{(i,j) \in E_1} \left( v_0^{-\frac{r(i,k),(j,l)}{2}} e^{-\frac{1}{2\sigma^2 v_0} (\theta_{ik} - \theta_{jl})^2} \right)^{q_{1,ij}^{\text{new}}}}{1}}. \quad (59)$$

The M-step can be derived in a standard way, and it has the same updates as in (54)-(55), with a new definition of  $F(\alpha, \theta; q_1, q_2)$  given by

$$\begin{aligned} F(\alpha, \theta; q_1, q_2) &= \|y - X_1(\alpha w + \theta)X_2\|^2 + \nu\alpha^2 \\ &+ \sum_{(i,j) \in E_1} \sum_{(k,l) \in E_2} \left( \frac{q_{1,ij}q_{2,kl}}{v_0} + \frac{1 - q_{1,ij}q_{2,kl}}{v_1} \right) (\theta_{ik} - \theta_{jl})^2. \end{aligned}$$

### 5.3 Applications in Biclustering

When both row and column graphs encode clustering structures discussed in Section 4.2, we have the biclustering model. In this section, we discuss both biclustering models induced by Kronecker and Cartesian products. We start with a special form of the likelihood (44), which is given by

$$y|\alpha, \theta, \sigma^2 \sim N(\alpha \mathbf{1}_{n_1} \mathbf{1}_{n_2}^T + \theta, \sigma^2 I_{n_1} \otimes I_{n_2}),$$

and the prior distribution on  $\alpha$  is given by (45). The prior distribution on  $\theta$  will be discussed in two cases.

**Cartesian product biclustering model.** Let  $k_1 \in [n_1]$  and  $k_2 \in [n_2]$  be upper bounds of the numbers of row and column clusters, respectively. We introduce two latent matrices  $\mu_1 \in \mathbb{R}^{k_1 \times n_2}$  and  $\mu_2 \in \mathbb{R}^{n_1 \times k_2}$  that serve as row and column clustering centers. The prior distribution is then specified by

$$\begin{aligned} p(\theta, \mu_1, \mu_2 | \gamma_1, \gamma_2, \sigma^2) &\propto \prod_{i=1}^{n_1} \prod_{j=1}^{k_1} \exp \left( -\frac{\|\theta_{i*} - \mu_{1,j*}\|^2}{2\sigma^2[v_0\gamma_{1,ij} + v_1(1 - \gamma_{1,ij})]} \right) \\ &\times \prod_{l=1}^{n_2} \prod_{h=1}^{k_2} \exp \left( -\frac{\|\theta_{*l} - \mu_{2,*h}\|^2}{2\sigma^2[v_0\gamma_{2,lh} + v_1(1 - \gamma_{2,lh})]} \right) \mathbb{I}\{\mathbf{1}_{n_1}^T \theta \mathbf{1}_{n_2} = 0\}, \end{aligned}$$

which can be regarded as an extension of (30) in the form of (46). The prior distributions on  $\gamma_1$  and  $\gamma_2$  are independently specified by (32) with  $(k, n)$  replaced by  $(k_1, n_1)$  and  $(k_2, n_2)$ . Finally,  $\sigma^2$  follows the inverse Gamma prior (6).

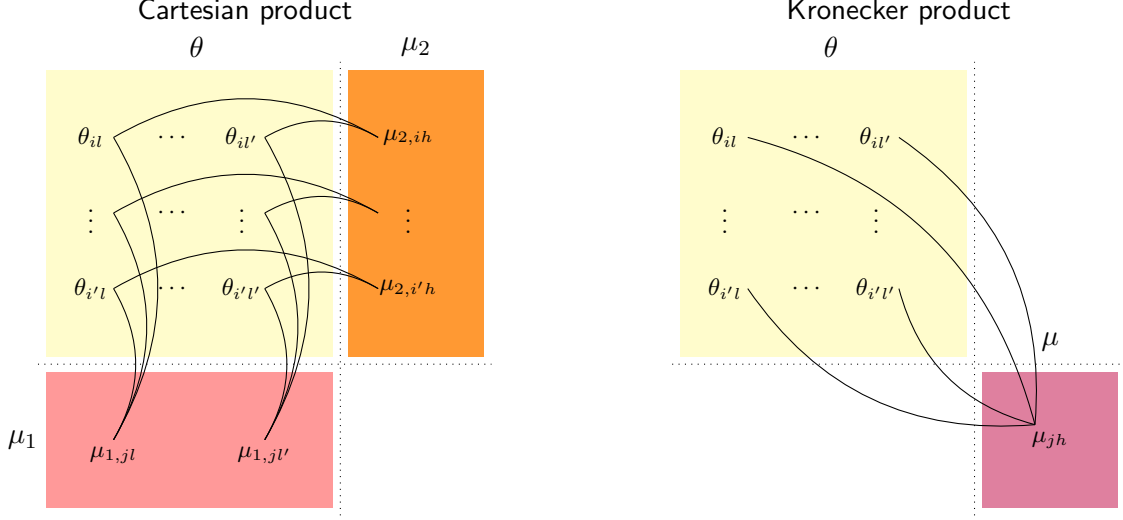


Figure 2: Structure diagrams for the two biclustering methods. The Cartesian product biclustering model (*Left*) and the Kronecker product biclustering model (*Right*) have different latent variables and base graphs. While the Cartesian product models the row and column clustering structures by separate latent variable matrices  $\mu_1 \in \mathbb{R}^{k_1 \times n_2}$  and  $\mu_2 \in \mathbb{R}^{n_1 \times k_2}$ , the Kronecker product directly models the checkerboard structure by a single latent matrix  $\mu \in \mathbb{R}^{k_1 \times k_2}$ .

We follow the framework of Section 3.2. The derivation of the EM algorithm requires lower bounding  $\log \sum_{T \in \text{spt}(G)} \sum_{e \in T} [v_0^{-1} \gamma_e + v_1^{-1} (1 - \gamma_e)]$ . Using the same argument in Section 5.1, we have the following lower bound

$$\sum_{i=1}^{n_1} \sum_{j=1}^{k_1} r_{1,ij} \log[v_0^{-1} \gamma_{1,ij} + v_1^{-1} (1 - \gamma_{1,ij})] + \sum_{l=1}^{n_2} \sum_{h=1}^{k_2} r_{2,lh} \log[v_0^{-1} \gamma_{2,lh} + v_1^{-1} (1 - \gamma_{2,lh})]. \quad (60)$$

By the symmetry of the complete bipartite graph,  $r_{1,ij}$  is a constant that does not depend on  $(i, j)$ . Then use the same argument in (34)-(35), and we obtain the fact that  $\sum_{i=1}^{n_1} \sum_{j=1}^{k_1} r_{1,ij} \log[v_0^{-1} \gamma_{1,ij} + v_1^{-1} (1 - \gamma_{1,ij})]$  is independent of  $\{\gamma_{1,ij}\}$ , and the same conclusion also applies to the second term of (60).

Since the lower bound (60) does not depend on  $\gamma_1, \gamma_2$ , the determinant factor in the density function  $p(\theta, \mu_1, \mu_2 | \gamma_1, \gamma_2, \sigma^2)$  does not play any role in the derivation of the EM algorithm. With some standard calculations, the E-step is given by

$$q_{1,ij}^{\text{new}} = \frac{\exp\left(-\frac{\|\theta_{i*} - \mu_{1,j*}\|^2}{2\sigma^2\bar{v}}\right)}{\sum_{u=1}^{k_1} \exp\left(-\frac{\|\theta_{i*} - \mu_{1,u*}\|^2}{2\sigma^2\bar{v}}\right)},$$

$$q_{1,lh}^{\text{new}} = \frac{\exp\left(-\frac{\|\theta_{*l} - \mu_{2,*h}\|^2}{2\sigma^2\bar{v}}\right)}{\sum_{v=1}^{k_2} \exp\left(-\frac{\|\theta_{*l} - \mu_{2,*v}\|^2}{2\sigma^2\bar{v}}\right)},$$

where  $\bar{v}^{-1} = v_0^{-1} - v_1^{-1}$ . The M-step is given by

$$\begin{aligned} (\alpha^{\text{new}}, \theta^{\text{new}}, \mu_1^{\text{new}}, \mu_2^{\text{new}}) &= \underset{\alpha, \mathbf{1}_{n_1}^T \theta \mathbf{1}_{n_2} = 0, \mu_1, \mu_2}{\text{argmin}} F(\alpha, \theta, \mu_1, \mu_2; q_1^{\text{new}}, q_2^{\text{new}}), \\ (\sigma^2)^{\text{new}} &= \frac{F(\alpha^{\text{new}}, \theta^{\text{new}}, \mu_1^{\text{new}}, \mu_2^{\text{new}}; q_1^{\text{new}}, q_2^{\text{new}}) + b}{2n_1 n_2 + n_1 k_2 + n_2 k_1 + a + 2}, \end{aligned}$$

where

$$\begin{aligned} F(\alpha, \theta, \mu_1, \mu_2; q_1, q_2) &= \|y - \alpha \mathbf{1}_{n_1} \mathbf{1}_{n_2}^T - \theta\|_F^2 + \nu \|\alpha\|^2 \\ &\quad + \sum_{i=1}^{n_1} \sum_{j=1}^{k_1} \left( \frac{q_{1,ij}}{v_0} + \frac{1 - q_{1,ij}}{v_1} \right) \|\theta_{i*} - \mu_{1,j*}\|^2 \\ &\quad + \sum_{l=1}^{n_2} \sum_{h=1}^{k_2} \left( \frac{q_{2,lh}}{v_0} + \frac{1 - q_{2,lh}}{v_1} \right) \|\theta_{*l} - \mu_{2,*h}\|^2. \end{aligned}$$

**Kronecker product biclustering model.** For the Kronecker product structure, we introduce a latent matrix  $\mu \in \mathbb{R}^{k_1 \times k_2}$ . Since the biclustering model implies a block-wise constant structure for  $\theta$ . Each entry of  $\mu$  serves as a center for a block of the matrix  $\theta$ . The prior distribution is defined by

$$p(\theta, \mu | \gamma_1, \gamma_2, \sigma^2) \propto \prod_{i=1}^{n_1} \prod_{j=1}^{k_1} \prod_{l=1}^{n_2} \prod_{h=1}^{k_2} \exp \left( - \frac{(\theta_{il} - \mu_{jh})^2}{2\sigma^2[v_0\gamma_{1,ij}\gamma_{2,lh} + v_1(1 - \gamma_{1,ij}\gamma_{2,lh})]} \right) \mathbb{I}\{\mathbf{1}_{n_1}^T \theta \mathbf{1}_{n_2} = 0\}.$$

The prior distribution is another extension of (30), and it is in a similar form of (56). To finish the Bayesian model specification, we consider the same priors for  $\gamma_1, \gamma_2, \sigma^2$  as in the Cartesian product case.

Recall that the lower bound of  $\log \sum_{T \in \text{spt}(G)} \sum_{e \in T} [v_0^{-1} \gamma_e + v_1^{-1} (1 - \gamma_e)]$  is given by (57) for a general Kronecker product structure. In the current setting, a similar argument gives the lower bound

$$\sum_{i=1}^{n_1} \sum_{j=1}^{k_1} \sum_{l=1}^{n_2} \sum_{h=1}^{k_2} r_{(i,l),(j,h)} \log[v_0^{-1} \gamma_{1,ij} \gamma_{2,lh} + v_1^{-1} (1 - \gamma_{1,ij} \gamma_{2,lh})].$$

Since  $r_{(i,l),(j,h)}$  is independent of  $(i, l), (j, h)$  by the symmetry of the complete bipartite graph, the above lower bound can be written as

$$\begin{aligned} & r \sum_{i=1}^{n_1} \sum_{j=1}^{k_1} \sum_{l=1}^{n_2} \sum_{h=1}^{k_2} \log[v_0^{-1} \gamma_{1,ij} \gamma_{2,lh} + v_1^{-1} (1 - \gamma_{1,ij} \gamma_{2,lh})] \\ &= r \log(v_0^{-1}) \sum_{i=1}^{n_1} \sum_{j=1}^{k_1} \sum_{l=1}^{n_2} \sum_{h=1}^{k_2} \gamma_{1,ij} \gamma_{2,lh} + r \log(v_1^{-1}) \sum_{i=1}^{n_1} \sum_{j=1}^{k_1} \sum_{l=1}^{n_2} \sum_{h=1}^{k_2} (1 - \gamma_{1,ij} \gamma_{2,lh}) \\ &= r n_1 n_2 \log(v_0^{-1}) + r n_1 n_2 (k_1 k_2 - 1) \log(v_1^{-1}), \end{aligned} \tag{61}$$

which is independent of  $\gamma_1, \gamma_2$ . The inequality (61) is because both  $\gamma_1$  and  $\gamma_2$  satisfy (31).

Again, the determinant factor in the density function  $p(\theta, \mu | \gamma_1, \gamma_2, \sigma^2)$  does not play any role in the derivation of the EM algorithm, because the lower bound (61) does not depend on  $(\gamma_1, \gamma_2)$ . Since we are working with the Kronecker product, we will derive a variational EM algorithm with the E-step finding the posterior distribution in the mean field class  $\mathcal{Q} = \{q(\gamma_1, \gamma_2) = q_1(\gamma_1)q_2(\gamma_2) : q_1, q_2\}$ . By following the same argument in Section 5.2, we obtain the E-step as

$$\begin{aligned} q_{1,ij}^{\text{new}} &= \frac{\exp\left(-\sum_{l=1}^{n_2} \sum_{h=1}^{k_2} \frac{q_{2,lh}(\theta_{il} - \mu_{jh})^2}{2\sigma^2 \bar{v}}\right)}{\sum_{u=1}^{k_1} \exp\left(-\sum_{l=1}^{n_2} \sum_{h=1}^{k_2} \frac{q_{2,lh}(\theta_{il} - \mu_{uh})^2}{2\sigma^2 \bar{v}}\right)}, \\ q_{2,lh}^{\text{new}} &= \frac{\exp\left(-\sum_{i=1}^{n_1} \sum_{j=1}^{k_1} \frac{q_{1,ij}^{\text{new}}(\theta_{il} - \mu_{jh})^2}{2\sigma^2 \bar{v}}\right)}{\sum_{v=1}^{k_2} \exp\left(-\sum_{i=1}^{n_1} \sum_{j=1}^{k_1} \frac{q_{1,ij}^{\text{new}}(\theta_{il} - \mu_{lv})^2}{2\sigma^2 \bar{v}}\right)} \end{aligned}$$

where  $\bar{v}^{-1} = v_0^{-1} - v_1^{-1}$ . The M-step is given by

$$\begin{aligned} (\alpha^{\text{new}}, \theta^{\text{new}}, \mu^{\text{new}}) &= \underset{\alpha, \mathbb{1}_{n_1}^T \theta \mathbb{1}_{n_2} = 0, \mu}{\operatorname{argmin}} F(\alpha, \theta, \mu; q_1^{\text{new}}, q_2^{\text{new}}), \\ (\sigma^2)^{\text{new}} &= \frac{F(\alpha^{\text{new}}, \theta^{\text{new}}, \mu^{\text{new}}; q_1^{\text{new}}, q_2^{\text{new}}) + b}{2n_1 n_2 + n_1 k_2 + n_2 k_1 + a + 2}, \end{aligned}$$

where

$$\begin{aligned} F(\alpha, \theta, \mu_1, \mu_2; q_1, q_2) &= \|y - \alpha \mathbb{1}_{n_1} \mathbb{1}_{n_2}^T - \theta\|_F^2 + \nu \|\alpha\|^2 \\ &\quad + \sum_{i=1}^{n_1} \sum_{j=1}^{k_1} \sum_{l=1}^{n_2} \sum_{h=1}^{k_2} \left( \frac{q_{1,ij} q_{2,lh}}{v_0} + \frac{1 - q_{1,ij} q_{2,lh}}{v_1} \right) (\theta_{il} - \mu_{jh})^2. \end{aligned}$$

## 6 Reduced Isotonic Regression

The models that we have discussed so far in our general framework all involve Gaussian likelihood functions and Gaussian priors. It is important to develop a natural extension of the framework to include non-Gaussian models. In this section, we discuss a reduced isotonic regression problem with a non-Gaussian prior distribution, while a full extension to non-Gaussian models will be considered as a future project.

Given a vector of observation  $y \in \mathbb{R}^n$ , the reduced isotonic regression seeks the best piecewise constant fit that is nondecreasing [38, 17]. It is an important model that has applications in problems with natural monotone constraint on the signal. With the likelihood  $y | \alpha, \theta, \sigma^2 \sim N(\alpha \mathbb{1}_n + \theta, \sigma^2 I_n)$ , we need to specify a prior distribution on  $\theta$  that induces both piecewise constant and isotonic structures. We propose the following prior distribution,

$$\theta | \gamma, \sigma^2 \sim p(\theta | \gamma, \sigma^2) \propto \prod_{i=1}^{n-1} \exp\left(-\frac{(\theta_{i+1} - \theta_i)^2}{2\sigma^2[v_0 \gamma_i + v_1(1 - \gamma_i)]}\right) \mathbb{I}\{\theta_i \leq \theta_{i+1}\} \mathbb{I}\{\mathbb{1}_n^T \theta = 0\}. \quad (62)$$

We call (62) the spike-and-slab half-Gaussian distribution. Note that the support of the distribution is the intersection of the cone  $\{\theta : \theta_1 \leq \theta_2 \leq \dots \leq \theta_n\}$  and the subspace  $\{\theta : \mathbf{1}_n^T \theta = 0\}$ . The parameters  $v_0$  and  $v_1$  play similar roles as in (3), which model the closeness between  $\theta_i$  and  $\theta_{i+1}$  depending on the value of  $\gamma_i$ .

**Proposition 6.1.** *For any  $\gamma \in \{0, 1\}^{n-1}$  and  $v_0, v_1 \in (0, \infty)$ , the spike-and-slab half-Gaussian prior (62) is well defined on  $\{\theta : \theta_1 \leq \theta_2 \leq \dots \leq \theta_n\} \cap \{\theta : \mathbf{1}_n^T \theta = 0\}$ , and its density function with respect to the Lebesgue measure restricted on the support is given by*

$$p(\theta|\gamma, \sigma^2) = 2^{n-1} \frac{1}{(2\pi\sigma^2)^{(n-1)/2}} \sqrt{n \prod_{i=1}^{n-1} [v_0^{-1}\gamma_i + v_1^{-1}(1-\gamma_i)]} \\ \times \exp\left(-\sum_{i=1}^{n-1} \frac{(\theta_{i+1} - \theta_i)^2}{2\sigma^2[v_0\gamma_i + v_1(1-\gamma_i)]}\right) \mathbb{I}\{\theta_1 \leq \theta_2 \leq \dots \leq \theta_n\} \mathbb{I}\{\mathbf{1}_n^T \theta = 0\}.$$

Note that the only place that Proposition 6.1 deviates from Proposition 2.1 is the extra factor  $2^{n-1}$  due to the isotonic constraint  $\{\theta : \theta_1 \leq \theta_2 \leq \dots \leq \theta_n\}$  and the symmetry of the density. We complete the model specification by put priors on  $\alpha, \gamma, \eta, \sigma^2$  that are given by (2), (4), (5) and (6).

Now we are ready to derive the EM algorithm. Since the base graph is a tree, the EM algorithm for reduced isotonic regression is exact. The E-step is given by

$$q_i^{\text{new}} = \frac{\eta\phi(\theta_i - \theta_{i-1}; 0, \sigma^2 v_0)}{\eta\phi(\theta_i - \theta_{i-1}; 0, \sigma^2 v_0) + (1 - \eta)\phi(\theta_i - \theta_{i-1}; 0, \sigma^2 v_1)}.$$

The M-step is given by

$$(\alpha^{\text{new}}, \theta^{\text{new}}) = \underset{\alpha, \theta_1 \leq \theta_2 \leq \dots \leq \theta_n, \mathbf{1}_n^T \theta = 0}{\operatorname{argmin}} F(\alpha, \theta; q^{\text{new}}), \quad (63)$$

where

$$F(\alpha, \theta; q) = \|y - \alpha \mathbf{1}_n - \theta\|^2 + \nu \alpha^2 + \sum_{i=1}^{n-1} \left( \frac{q_i}{v_0} + \frac{1 - q_i}{v_1} \right) (\theta_i - \theta_{i-1})^2,$$

and the updates of  $\sigma^2$  and  $\eta$  are given by (17) with  $p = n$ . The M-step (63) can be solved by a very efficient optimization technique. Since  $\|y - \alpha \mathbf{1}_n - \theta\|^2 = \|(\bar{y} - \alpha) \mathbf{1}_n\|^2 + \|y - \bar{y} \mathbf{1}_n - \theta\|^2$  by  $\mathbf{1}_n^T \theta = 0$ ,  $\alpha$  and  $\theta$  can be updated independently. It is easy to see that  $\alpha^{\text{new}} = \frac{n}{n+\nu} \bar{y}$ . The update of  $\theta$  can be solved by SPAVA [6].

Similar to the Gaussian case, the parameter  $v_0$  determines the complexity of the model. For each  $v_0$  between 0 and  $v_1$ , we apply the EM algorithm above to calculate  $\hat{q}$ , and then let  $\hat{\gamma}_i = \hat{\gamma}_i(v_0) = \mathbb{I}\{\hat{q}_i \geq 1/2\}$  form a solution path. The best model will be selected from the EM-solution path by the limiting version of the posterior distribution as  $v_0 \rightarrow 0$ .

Given a  $\gamma \in \{0, 1\}^{n-1}$ , we write  $s = 1 + \sum_{i=1}^{n-1} (1 - \gamma_i)$  to be the number of pieces, and  $Z_\gamma \in \{0, 1\}^{n \times s}$  is the membership matrix defined in Section 3.3. As  $v_0 \rightarrow 0$ , a slight

variation of Proposition 3.1 implies that  $\theta$  that follows (62) weakly converges to  $Z_\gamma \tilde{\theta}$ , where  $\tilde{\theta}$  is distributed by

$$p(\tilde{\theta}|\gamma, \sigma^2) \propto \exp\left(-\sum_{l=1}^s \frac{(\tilde{\theta}_l - \tilde{\theta}_{l+1})^2}{2\sigma^2 v_1}\right) \mathbb{I}\{\tilde{\theta}_1 \leq \tilde{\theta}_2 \leq \dots \leq \tilde{\theta}_s\} \mathbb{I}\{\mathbf{1}_n^T Z_\gamma \tilde{\theta} = 0\}. \quad (64)$$

The following proposition determines the normalizing constant of the above distribution.

**Proposition 6.2.** *The density function of (64) is given by*

$$p(\tilde{\theta}|\gamma, \sigma^2) = 2^{s-1} (2\pi\sigma^2)^{-(s-1)/2} \sqrt{\det_{Z_\gamma^T \mathbf{1}_n} (Z_\gamma^T \tilde{L}_\gamma Z_\gamma)} \times \\ \exp\left(-\sum_{l=1}^s \frac{(\tilde{\theta}_l - \tilde{\theta}_{l+1})^2}{2\sigma^2 v_1}\right) \mathbb{I}\{\tilde{\theta}_1 \leq \tilde{\theta}_2 \leq \dots \leq \tilde{\theta}_s\} \mathbb{I}\{\mathbf{1}_n^T Z_\gamma \tilde{\theta} = 0\}, \quad (65)$$

where  $Z_\gamma$  and  $\tilde{L}_\gamma$  are defined in Section 3.3.

Interestingly, compared with the formula (22), (65) has an extra  $2^{s-1}$  due to the isotonic constraint  $\{\tilde{\theta}_1 \leq \dots \leq \tilde{\theta}_s\}$ .

Following Section 3.3, we consider a reduced version of the likelihood  $y|\alpha, \tilde{\theta}, \gamma, \sigma^2 \sim N(\alpha \mathbf{1}_n + Z_\gamma \tilde{\theta}, \sigma^2 I_n)$ . Then, with the prior distributions on  $\alpha, \tilde{\theta}, \gamma, \sigma^2$  specified by (2), (65), (4), (5) and (6), we obtain the joint posterior distribution  $p(\alpha, \tilde{\theta}, \gamma, \sigma^2|y)$ . Ideally, we would like to integrate out  $\alpha, \tilde{\theta}, \sigma^2$  and use  $p(\gamma|y)$  for model selection. However, the integration with respect to  $\tilde{\theta}$  is intractable due to the isotonic constraint. Therefore, we propose to maximize out  $\alpha, \tilde{\theta}, \sigma^2$ , and then the model selection score for reduced isotonic regression is given by

$$g(\gamma) = \max_{\alpha, \tilde{\theta}_1 \leq \dots \leq \tilde{\theta}_s, \mathbf{1}_n^T Z_\gamma \tilde{\theta} = 0, \sigma^2} \log p(\alpha, \tilde{\theta}, \gamma, \sigma^2|y).$$

For each  $\gamma$ , the optimization involved in the evaluation of  $g(\gamma)$  can be done efficiently, which is very similar to the M-step updates.

## 7 Numerical Results

In this section, we test the performance of the methods proposed in the paper and compare the accuracy in terms of sparse signal recovery and graphical structure estimation with existing methods. We name our method BayesMSG (Bayesian Model Selection on Graphs) throughout the section. All simulation studies and real data applications were conducted on a standard laptop (2.6 GHz Intel Core i7 processor and 16GB memory) using R/Julia programming language. Detailed codes for implementation of the algorithm are available online at <https://github.com/youngseok-kim/BayesMSG-paper> for reproduction of the results.

Our Bayesian method outputs a subgraph defined by

$$\hat{\gamma} = \operatorname{argmax} \{g(\gamma) : \gamma \in \{\hat{\gamma}(v_0)\}_{0 < v_0 \leq v_1}\},$$

which is a sub-model selected by the model selection score  $g(\gamma)$  on the EM solution path (see Section 3.3 for details). Suppose  $\gamma^*$  is the underlying true subgraph that generates the data, we measure the performance of  $\hat{\gamma}$  by false discovery proportion and power. The definitions are

$$\text{FDP} = \frac{\sum_{(i,j) \in E} (1 - \hat{\gamma}_{ij}) \gamma_{ij}^*}{\sum_{(i,j) \in E} (1 - \hat{\gamma}_{ij})} \quad \text{and} \quad \text{POW} = 1 - \frac{\sum_{(i,j) \in E} (1 - \gamma_{ij}^*) \hat{\gamma}_{ij}}{\sum_{(i,j) \in E} (1 - \gamma_{ij}^*)},$$

where we adopt the convention that  $0/0 = 1$ . Note that the above FDP and POW are not suitable for the clustering/biclustering model, because clustering structures are equivalent up to arbitrary clustering label permutations.

The sub-model indexed by  $\hat{\gamma}$  also induces a point estimator. This can be done by calculating the posterior mean of the reduced model specified by the likelihood (24) and priors (2) and (22). With notations  $p(y|\alpha, \tilde{\theta}, \gamma, \sigma^2)$ ,  $p(\alpha|\sigma^2)$  and  $p(\tilde{\theta}|\gamma, \sigma^2)$  for (24), (2) and (22), the point estimator is defined by  $\hat{\beta} = \alpha^{\text{est}} w + Z_{\hat{\gamma}} \tilde{\theta}^{\text{est}}$ , where  $Z_{\gamma}$  is the membership matrix defined in Section 3.3, and the definition of  $(\alpha^{\text{est}}, \tilde{\theta}^{\text{est}})$  is given by

$$(\alpha^{\text{est}}, \tilde{\theta}^{\text{est}}) = \underset{\alpha, \tilde{\theta} \in \{\tilde{\theta}: w^T Z_{\hat{\gamma}} \tilde{\theta} = 0\}}{\text{argmax}} \log \left[ p(y|\alpha, \tilde{\theta}, \hat{\gamma}, \sigma^2) p(\alpha|\sigma^2) p(\tilde{\theta}|\hat{\gamma}, \sigma^2) \right],$$

which is a simple quadratic programming whose solution does not depend on  $\sigma^2$ . Note that the definition implies that  $\hat{\beta}$  is the posterior mode of the reduced model. Since the posterior distribution is Gaussian,  $\hat{\beta}$  is also the posterior mean. The performance of  $\hat{\beta}$  will be measured by the mean squared error

$$\text{MSE} = \frac{1}{n} \|X(\hat{\beta} - \beta^*)\|^2,$$

where  $\beta^*$  is the true parameter that generates the data.

The hyper-parameters  $a, b, A, B$  in (5) and (6) are all set as the default value 1. The same rule is also applied to the extensions in Sections 4-6.

## 7.1 Simulation Studies

In this section, we compare the proposed Bayesian methods with two popular methods in the literature. The first method is the generalized Lasso [45, 39, 46], defined by

$$\hat{\beta} = \frac{1}{2} \|y - X\beta\|^2 + \lambda \sum_{(i,j) \in E} |\beta_i - \beta_j|. \quad (66)$$

The second method is the  $\ell_0$ -penalized least-squares [2, 15, 13], defined by

$$\hat{\beta} = \frac{1}{2} \|y - X\beta\|^2 + \lambda \sum_{(i,j) \in E} \mathbb{I}\{\beta_i \neq \beta_j\}. \quad (67)$$

For both methods, an estimated subgraph is given by

$$\hat{\gamma}_{ij} = \mathbb{I}\{|\hat{\beta}_i - \hat{\beta}_j| \leq \epsilon\},$$

for all  $(i, j) \in E$ . Here, the number  $\epsilon$  is taken as  $10^{-8}$ . The two methods are referred to by GenLasso and  $\ell_0$ -pen from now on.

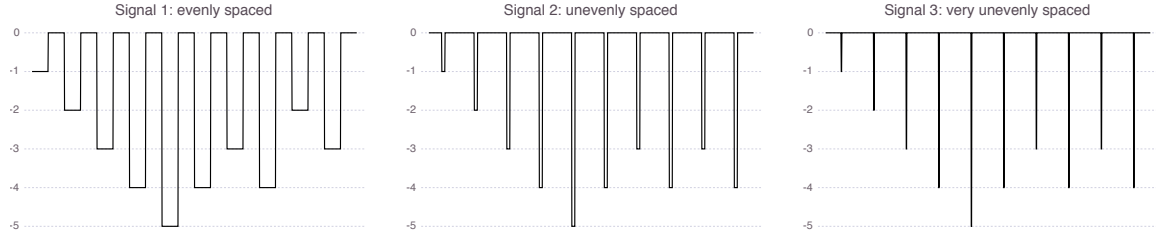


Figure 3: Three different signals for the linear chain graph. All signals have 20 pieces. Signal 1 has evenly spaced changes (each piece has length 50), Signal 2 has unevenly spaced changes (a smaller piece has length 10), and Signal 3 has very unevenly spaced changes (a smaller one has length 2).

### 7.1.1 Linear Chain Graph

We first consider the simplest linear chain graph, which corresponds to the change-point model explained in Example 2.2. We generate data according to  $y \sim N(\beta^*, \sigma^2 I_n)$  with  $n = 1000$  and  $\sigma \in \{0.1, 0.2, 0.3, 0.4, 0.5\}$ . The mean vector  $\beta^* \in \mathbb{R}^n$  is specified in three different cases as shown in Figure 3. We compare the performances of the proposed Bayesian method, GenLasso and  $\ell_0$ -pen. For the linear chain graph, GenLasso is the same as fused Lasso [45]. Its tuning parameter  $\lambda$  in (66) is selected by cross validation using the default method of the R package `genlasso` [1]. For  $\ell_0$ -pen, the  $\lambda$  in (67) is selected using the method suggested by [13].

Table 1: Comparisons of the three methods for the linear chain graph.

	$\sigma$	Even			Uneven			Very uneven		
		MSE	FDP	POW	MSE	FDP	POW	MSE	FDP	POW
BayesMSG	0.1	0.00019	0.00	1.00	0.00949	0.00	1.00	0.00217	0.00	0.80
	0.2	0.00585	0.00	0.98	0.01010	0.00	0.97	0.00279	0.00	0.81
	0.3	0.01620	0.01	0.96	0.01116	0.01	0.97	0.00349	0.00	0.81
	0.4	0.01940	0.05	0.95	0.01693	0.02	0.96	0.00837	0.00	0.79
	0.5	0.04667	0.10	0.95	0.03682	0.02	0.96	0.01803	0.05	0.78
GenLasso	0.1	0.00094	0.81	1.00	0.00116	0.90	1.00	0.00570	0.96	1.00
	0.2	0.00374	0.81	1.00	0.00458	0.90	1.00	0.01152	0.94	1.00
	0.3	0.00842	0.81	0.98	0.01024	0.89	1.00	0.02084	0.93	0.99
	0.4	0.01494	0.81	0.98	0.01813	0.88	0.98	0.03376	0.92	0.98
	0.5	0.02345	0.82	0.98	0.02818	0.89	0.98	0.04984	0.92	0.97
$\ell_0$ -pen	0.1	0.00505	0.00	0.98	0.00288	0.00	0.97	0.02042	0.00	0.81
	0.2	0.00545	0.00	0.98	0.00888	0.00	0.94	0.06049	0.00	0.63
	0.3	0.00399	0.01	0.98	0.00918	0.02	0.94	0.06121	0.00	0.63
	0.4	0.00826	0.02	0.97	0.01119	0.02	0.93	0.06250	0.00	0.63
	0.5	0.06512	0.03	0.92	0.04627	0.02	0.93	0.06452	0.00	0.63

The results are summarized in Table 1. Some typical solutions of the three methods are plotted in Figure 4. In terms of MSE, our Bayesian method achieves the smallest error among the three methods when  $\sigma$  is small, and GenLasso has the best performance when  $\sigma$  is large. For model selection performance measured by FDP and POW, the Bayesian method is the

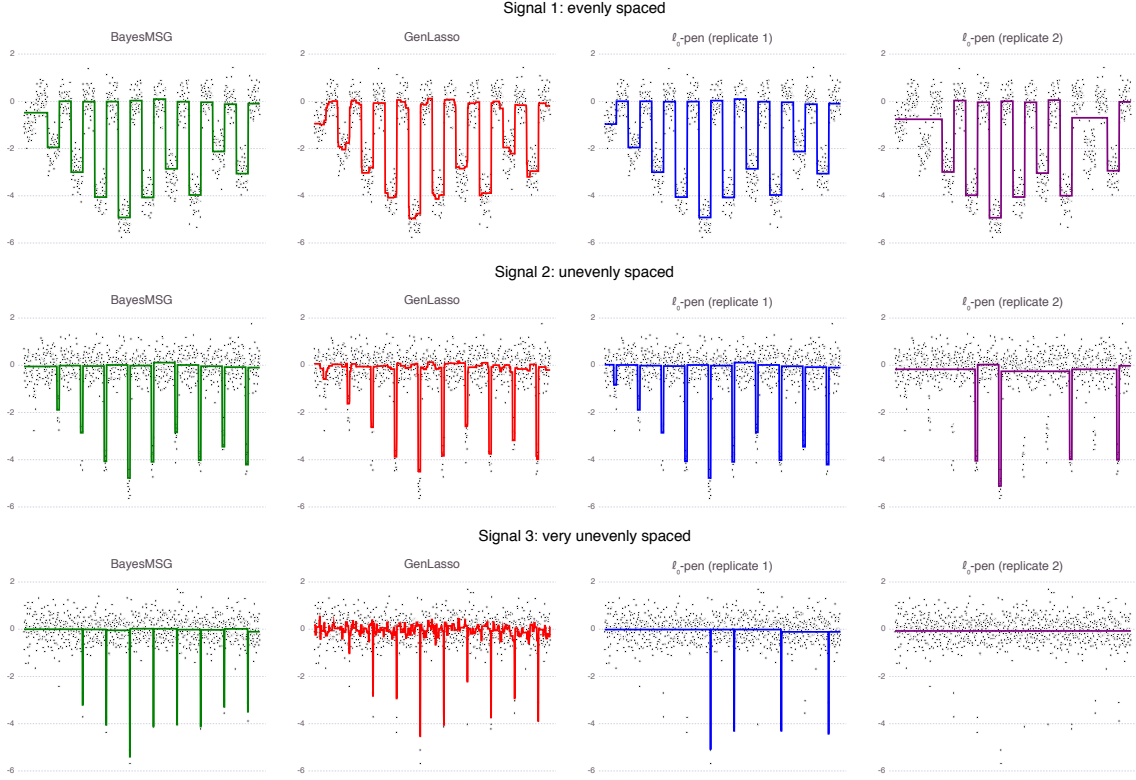


Figure 4: Visualization of typical solutions of the three methods when  $\sigma = 0.5$ . Since  $\ell_0$ -pen is very unstable, we plot contrasting solutions from two independent replicates. (Top) Evenly spaced signal; (Center) Unequally spaced signal; (Bottom) Very unevenly spaced signal; (Far Left) BayesMSG; (Left) GenLasso; (Right and Far Right) Two independent replicates of  $\ell_0$ -pen.

best, and  $\ell_0$ -pen is better than GenLasso. We also point out that the solutions of  $\ell_0$ -pen is highly unstable, as shown in Figure 4.

### 7.1.2 Two-Dimensional Grid Graph

We consider the two-dimensional grid graph described in Example 2.3. The data is generated according to  $y_{ij} \sim N(\kappa\mu_{ij}^*, 1)$  for  $i = 1, \dots, 21$  and  $j = 1, \dots, 21$ , where

$$\mu_{ij}^* = \left\lceil 2.8 \cos \left( \frac{\sqrt{i^2 + j^2}}{2\pi} \right) - 0.2 \right\rceil,$$

and  $\kappa \in \{1, 2, \dots, 10\}$  is used to control the signal strength. Note that  $\mu_{ij}^*$  has a piecewise constant structure because of the operation by  $\lceil \cdot \rceil$  that denotes the integer part. In fact,  $\mu_{ij}^*$  only takes 5 possible values as shown in Figure 6.

Since the R package `genlasso` does not provide a tuning method for the  $\lambda$  in (66) for the two-dimensional grid graph setting, we report MSE based on the  $\lambda$  selected by cross validation, and FDP and POW are reported based on the  $\lambda$  that minimizes the FDP. The  $\lambda$  in  $\ell_0$ -pen is tuned by the method in [13].

The results are shown in Figure 5. It is clear that our method outperforms the other two. We also illustrate the solution path of our method in Figure 6. Typical solutions of GenLasso and  $\ell_0$ -pen are visualized in Figure 7. We observe that  $\ell_0$ -pen tends to oversmooth the data, while GenLasso tends to undersmooth.

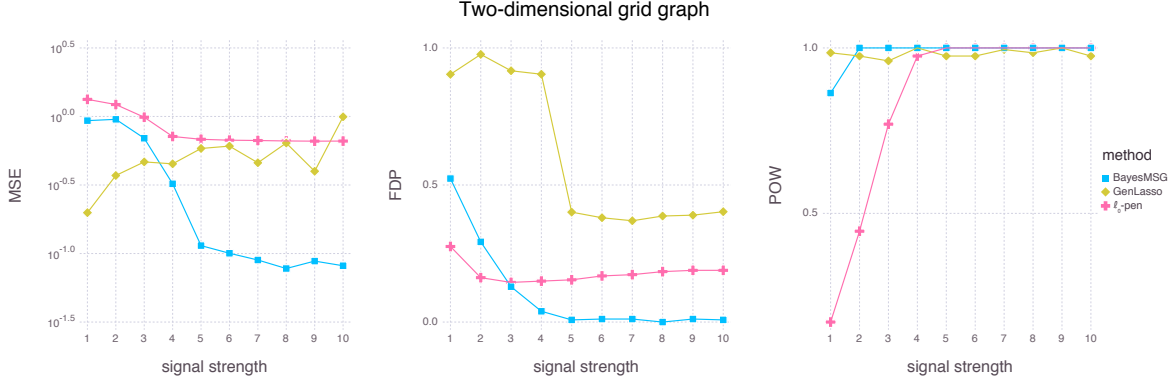


Figure 5: Comparisons of the three methods for the two-dimensional grid graph. (Left) MSE; (Center) FDP; (Right) POW.

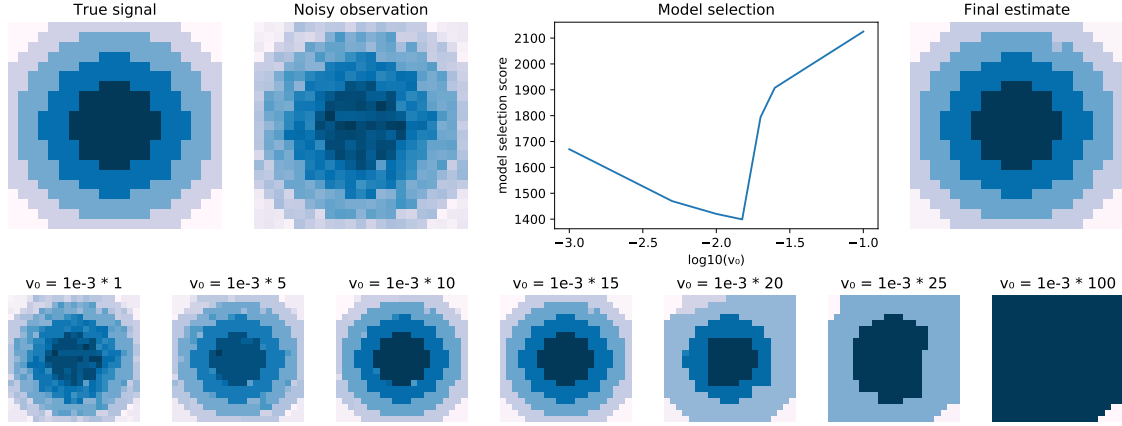


Figure 6: (Top panels) True signal, noisy observations, model selection score, and final estimate; (Bottom panels) A regularization path from  $v_0 = 10^{-3}$  to  $v_0 = 10^{-1}$ .

### 7.1.3 Generic Graphs

In this section, we consider some graphical structures that naturally arise in real world applications. The three graphs to be tested are the Chicago metropolitan area road network<sup>1</sup>,

<sup>1</sup><http://www.cs.utah.edu/~lifeifei/SpatialDataset.htm>

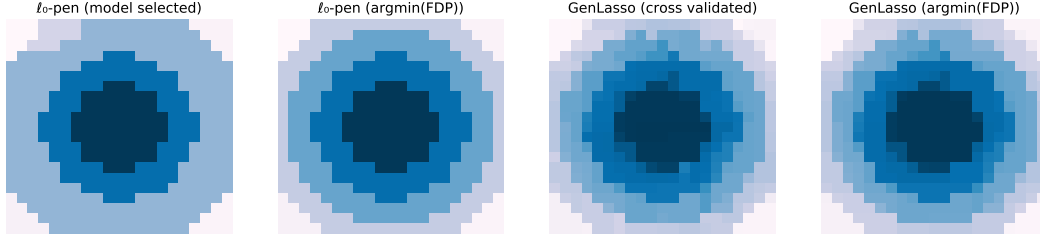


Figure 7: (Far Left)  $\ell_0$ -pen with  $\lambda$  selected using the method in [13]; (Left)  $\ell_0$ -pen with  $\lambda$  that minimizes FDP; (Right) GenLasso with  $\lambda$  selected by cross validation; (Far Right) GenLasso with  $\lambda$  that minimizes FDP.

the Enron email network<sup>2</sup>, and the Facebook egonet network<sup>3</sup>. For all the three networks, we extract induced subgraphs of sizes about 4000. Graph properties for the three networks are summarized in Table 2. For each network, we calculate its number of nodes, number of edges, mean and standard deviation of effective resistances, diameter, and number of connected components. We observe that the three networks behave very differently. The Chicago roadmap network is locally and globally tree-like, since its number of edges is very close to its number of nodes, and the distribution of its effective resistances highly concentrates around 1. The other two networks, the Enron email network and the Facebook egonet, are denser graphs but their effective resistances behave in very different ways.

Table 2: Graph properties of the three real networks.

Name	# of nodes	# of edges	mean.ER	sd.ER	diameter	# of CC
Chicago roadmap	4126	4308	0.9575	0.0499	324	1
Enron email	4112	14520	0.2831	0.2341	14	1
Facebook egonet	4039	88234	0.0457	0.0608	8	1

Table 3: Important features of the signals on the three networks.

Name	# of clust	# of nodes in each clusters	# of cuts	total variation
Chicago roadmap	4	(576, 678, 835, 2037)	31	$31 \times \kappa$
Enron email	4	(384, 538, 1531, 1659)	4570	$5047 \times \kappa$
Facebook egonet	4	(750, 753, 778, 1758)	651	$1220 \times \kappa$

For each network, we generate data according to  $y_i \sim N(\kappa\mu_i^*, 1)$  on its set of nodes, with the signal strength varies according to  $\kappa \in \{1, 2, \dots, 5\}$ . The signal  $\mu^*$  for each graph is generated as follows:

1. Pick four anchor nodes from the the set of all nodes uniformly at random.

<sup>2</sup><http://snap.stanford.edu/data/email-Enron.html>

<sup>3</sup><http://snap.stanford.edu/data/ego-Facebook.html>

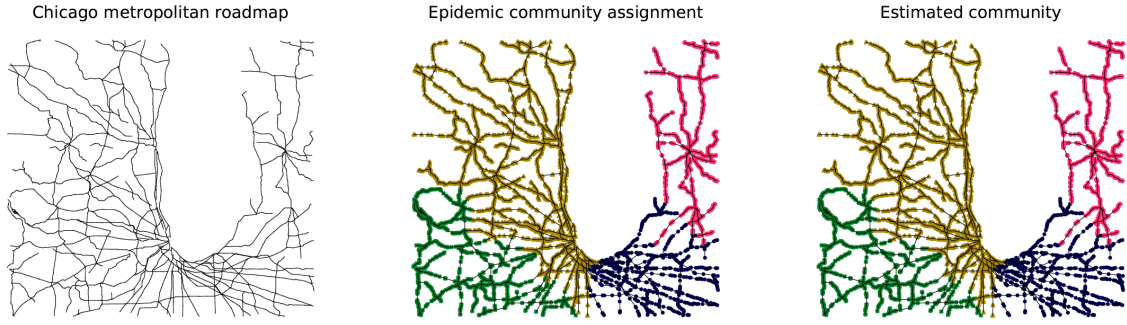


Figure 8: The Chicago roadmap network with signals exhibiting four clusters.

2. For each node, compute the length of the shortest path to each of the four anchor nodes.
3. Code the  $i$ th node by  $j$  if the  $j$ th anchor node is the closest one to the  $i$ th node. This gives four clusters for each graph.
4. Generate a piecewise constant signal  $\mu_i^* = j$ .

Some properties of the signals are summarized in Table 3, where the number of cuts of  $\mu^*$  with respect to the base graph  $G = (V, E)$  is defined by  $\sum_{(i,j) \in E} \mathbb{I}\{\mu_i^* \neq \mu_j^*\}$ , and the total variation of  $\mu^*$  means  $\sum_{(i,j) \in E} |\mu_i^* - \mu_j^*|$ . We also plot the signal on the Chicago roadmap network in Figure 8.

Since the R package `genlasso` does not provide a tuning method for the  $\lambda$  in (66) for a generic graph, we report MSE based on the  $\lambda$  selected by cross validation, and FDP and POW are reported based on the  $\lambda$  that minimizes the FDP. The  $\lambda$  in  $\ell_0$ -pen is tuned by the method in [13].

The results are shown in Figure 9. It is clear that our method outperforms the other two. When the signal strength  $\kappa$  is small, we observe that GenLasso sometimes has the smallest MSE, but its MSE grows very quickly as  $\kappa$  increases. For most  $\kappa$ 's, our method and  $\ell_0$ -pen are similar in terms of MSE. In terms of the model selection performance, GenLasso is not competitive, and our method outperforms  $\ell_0$ -pen.

#### 7.1.4 Comparisons of Different Graphs

One key ingredient of our Bayesian model selection framework is the specification of the base graph. For the same problem, there can be multiple ways to specify the base graph that lead to completely different models and methods. In this section, we consider an example and compare the performances of different Bayesian methods with different base graphs.

We consider observations  $y_{ij} \sim N(\beta_{ij}^*, 1)$  for  $i \in [n_1]$  and  $j \in [n_2]$ . We fix  $n_2 = 12$  and vary  $n_1$  from 24 to 144. The signal matrix  $\beta^* \in \mathbb{R}^{n_1 \times n_2}$  has a checkerboard structure as shown in Figure 10. That is, the  $n_1 \times n_2$  matrix is divided into  $6 \times 6$  equal-sized blocks. On the  $(u, v)$ th block,  $\beta_{ij}^* = 2(u + v - 6)$ .

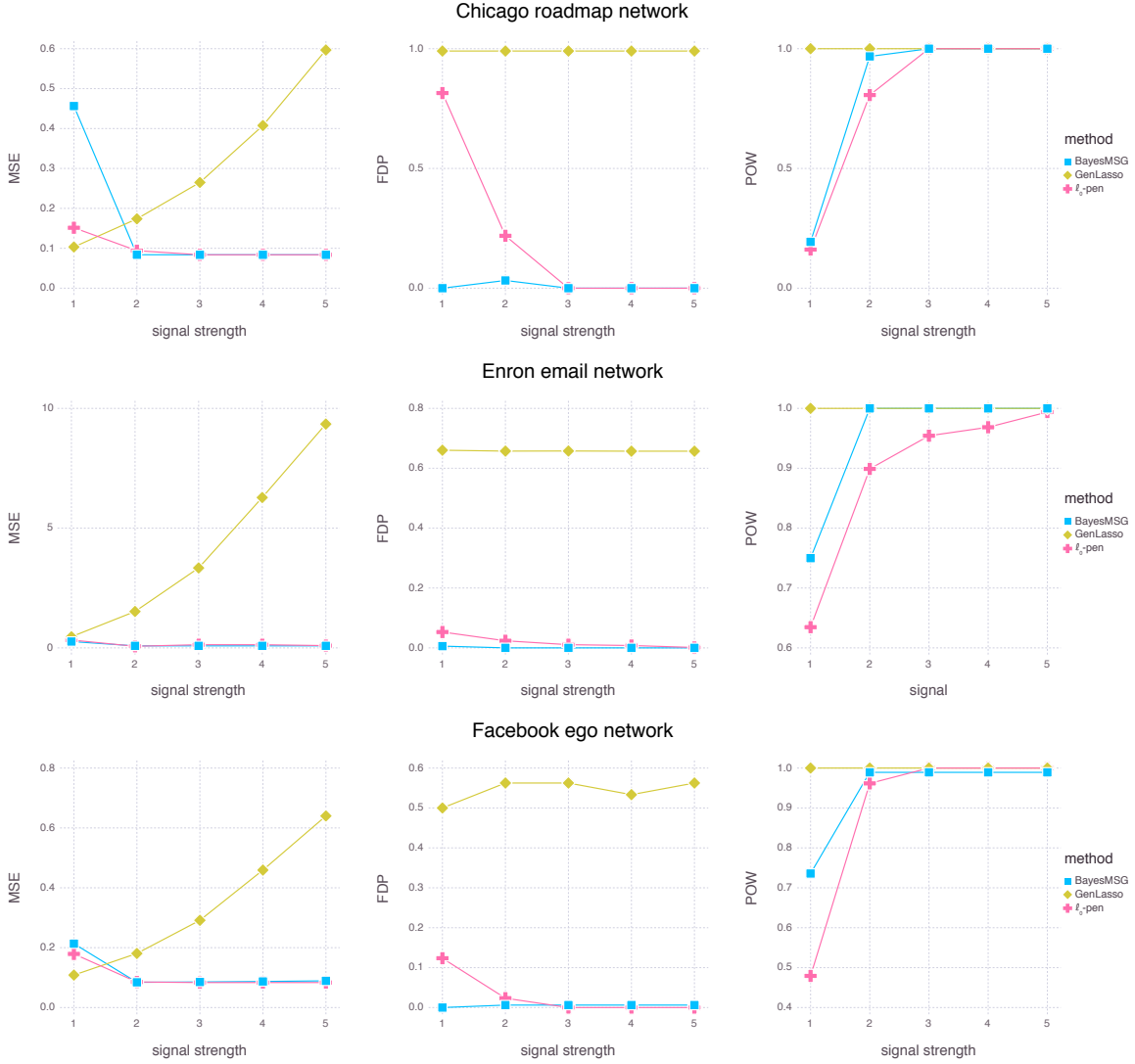


Figure 9: Comparison of the three methods on generic graphs. (Top) Chicago Roadmap network; (Center) Enron Email network; (Bottom) Facebook Ego network.

The following models are considered to fit the observations:

1. *Vector clustering.* We regard the matrix  $y \in \mathbb{R}^{n_1 \times n_2}$  as a  $n_1 n_2$ -dimensional vector and apply the clustering model described in Section 4.2 with  $n = k = n_1 n_2$ .
2. *Two-dimensional grid graph.* The two-dimensional image denoising model described in Example 2.3 is fit to the observations.
3. *Row clustering.* We regard the matrix  $y \in \mathbb{R}^{n_1 \times n_2}$  as  $n = n_1$  observations in  $\mathbb{R}^d$  with  $d = n_2$ , and then fit the clustering model described in Section 4.2 to the rows of  $y$  with  $n = k = n_1$ .

4. *Cartesian product biclustering.* The biclustering model induced by the Cartesian product described in Section 5.3 is fit to the observations.
5. *Kronecker product biclustering.* The biclustering model induced by the Kronecker product described in Section 5.3 is fit to the observations.

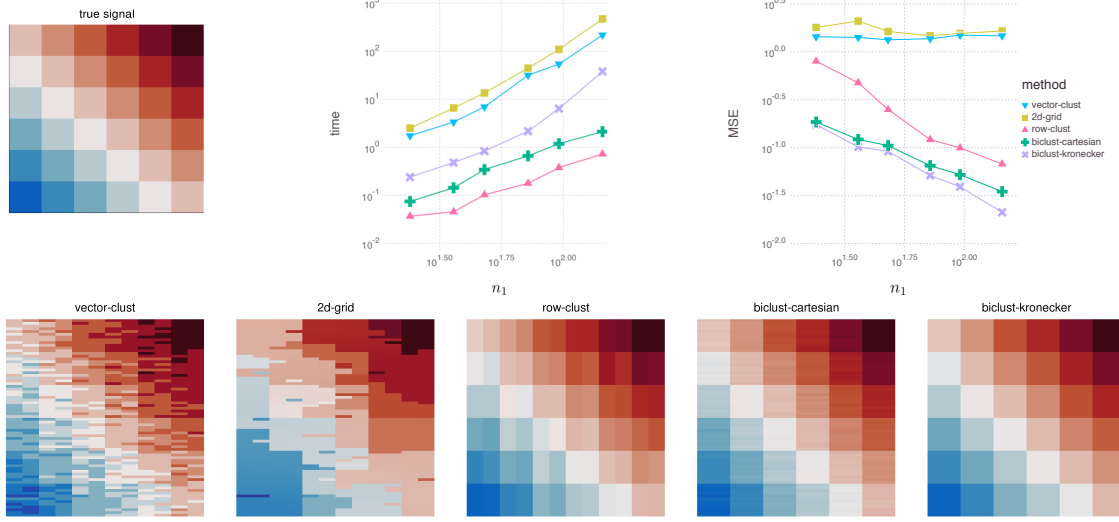


Figure 10: (Top left) True signal; (Top center) Computational time; (Top right) MSE; (Bottom) Heatmaps of estimators using different models ( $n_1 = 72$ ).

Figure 10 summarizes the results. In terms of MSE, the vector clustering and the two-dimensional grid graph do not fully capture the structure of the data and thus perform worse than all other methods. Both the biclustering models are designed for the checkerboard structure, and they therefore have the best performances. Between the two biclustering models, the one induced by the Kronecker product has a smaller MSE at the cost of a higher computational time.

To summarize the comparisons, we would like to emphasize that the right choice of the base graph has an enormous impact to the result. This also highlights the flexibility of our Bayesian model selection framework that is able to capture various degrees of structures of the data.

## 7.2 Real Data Applications

In this section, we apply our methods to three different data sets.

**Global warming data.** The global warming data has been studied previously by [51, 47]. It consists of 166 data points in degree Celsius from 1850 to 2015. Here we fit the Bayesian reduced isotonic regression discussed in Section 6. Our results are shown in Figure 11. When

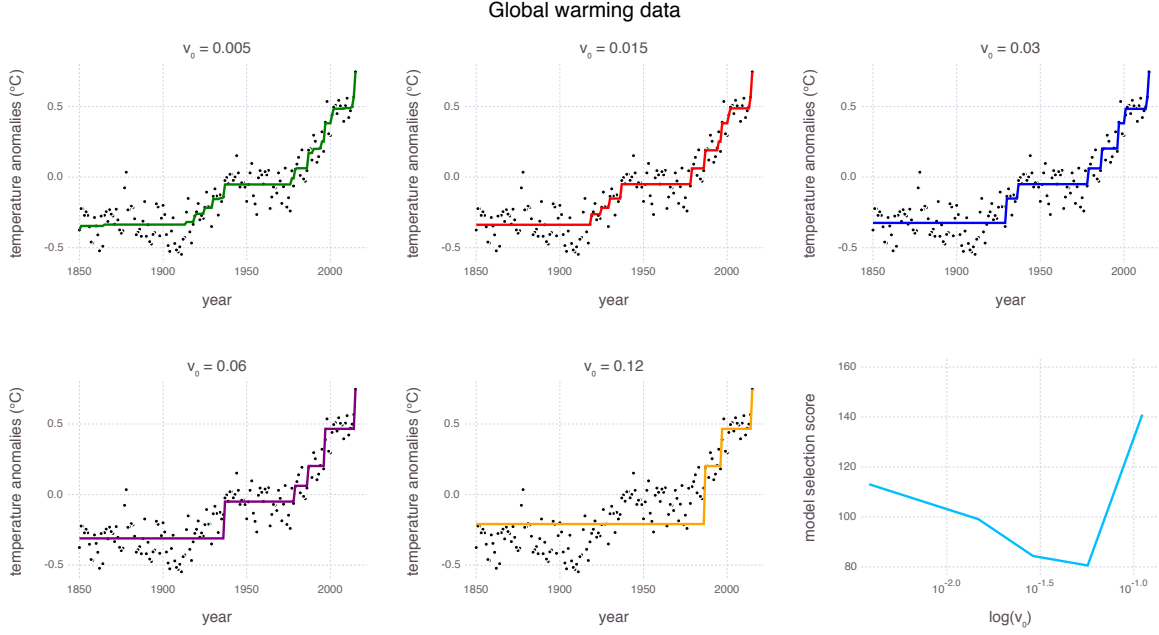


Figure 11: Solution path for Bayesian reduced isotonic regression.

$v_0$  is nearly zero, the solution is very close to the regular isotonic regression that can be solved efficiently by the pool-adjacent-violators algorithm (PAVA) [33]. When  $v_0 = 0.005$ , we obtain a fit with 24 pieces. The PAVA outputs a very similar fit also with 24 pieces. In contrast, the Bayesian model selection procedure suggests a model with  $v_0 = 0.06$ , which has only 6 pieces, a significantly more parsimonious and a more interpretable fit. This may suggest global warming is accelerating faster in recent years. The same conclusion cannot be obtained from the suboptimal fit with 24 pieces.

**Lung cancer data.** We illustrate the Bayesian biclustering models by a gene expression data set from a lung cancer study. The same data set has also been used by [4, 27, 40, 8]. Following [8], we study a subset with 56 samples and 100 genes. The 56 samples comprise 20 pulmonary carcinoid samples (Carcinoid), 13 colon cancer metastasis samples (Colon), 17 normal lung samples (Normal) and 6 small cell lung carcinoma samples (SmallCell). We also apply the row and column normalizations as has been done in [8].

Our goal is to identify sets of biologically relevant genes, for example, that are significantly expressed for certain cancer types. We fit both Bayesian biclustering models (Section 5.3) induced by the Cartesian and Kronecker products to the data with  $n_1 = 56$ ,  $n_2 = 100$ ,  $k_1 = 10$ , and  $k_2 = 20$ . Recall that  $k_1$  and  $k_2$  are upper bounds of the numbers of row and column clusters, and the actual numbers of row and column clusters will be learned

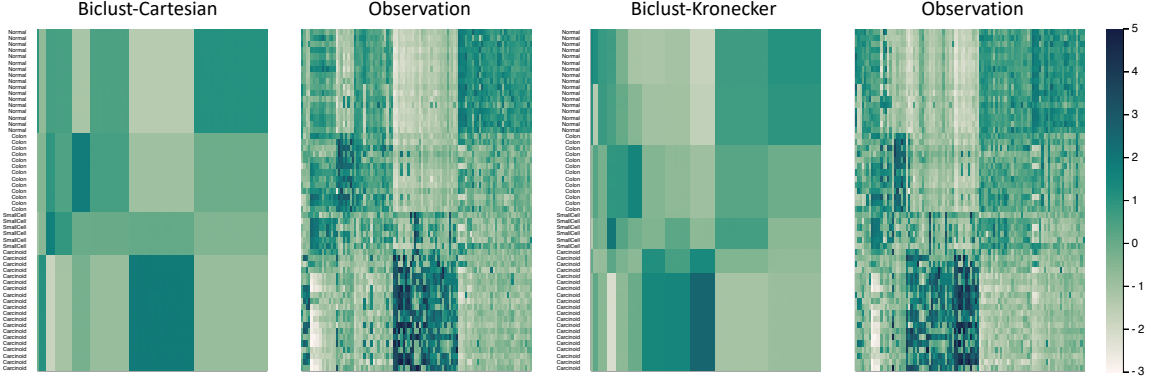


Figure 12: Results of biclustering for the lung cancer data. The rows of the four heatmaps are ordered in the same way according to the labels of tumor types. The columns of the first two heatmaps on the left are ordered according to the clustering labels of the Bayesian Cartesian biclustering method. The columns of the other two heatmaps on the right are ordered according to the clustering labels of the Bayesian Kronecker biclustering method.

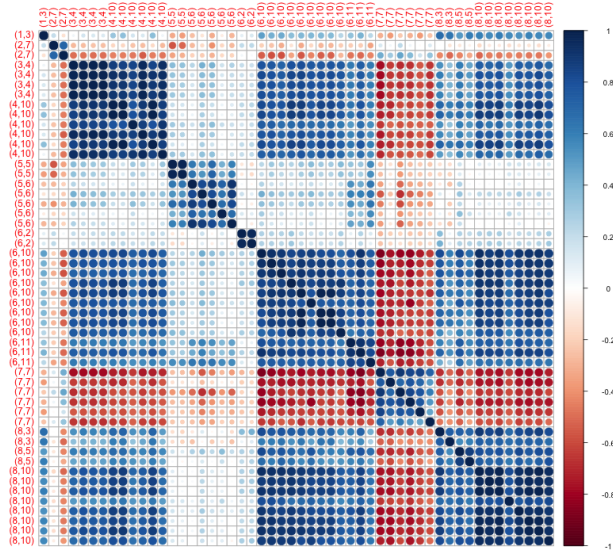


Figure 13: A correlation plot of the selected genes.

through Bayesian model selection. To pursue a more flexible procedure of model selection, we use two independent pairs of  $(v_0, v_1)$  for the row structure and the column structure. To be specific, let  $(v_0, v_1)$  be the parameters for the row structure, and the parameters for the column structure are set as  $(cv_0, cv_1)$  with some  $c \in \{1/10, 1/5, 1/2, 1, 2, 5, 10\}$ . Then, the model selection scores are computed with both  $v_0$  and  $c$  varying in their ranges.

The results are shown in Figure 12. The two methods select different models with different interpretations. The Cartesian product fit gives 4 row clusters and 8 column clusters, while the Kronecker product fit gives 6 row clusters and 11 column clusters. Even though we have

not used the information of the row labels for both biclustering methods, the row clustering structure output by the Cartesian product model almost coincides with these labels except one. On the other hand, the Kronecker product model leads to a finer row clustering structure, with potential discoveries of subtypes of both normal lung samples and pulmonary carcinoid samples.

An important goal of biclustering is to simultaneously identify gene and tumor types. To be specific, we seek to find genes that show different expression levels for different types of samples. To this end, we report those genes that are clustered together by both the Cartesian and Kronecker product structures. Groups of genes with size between 2 and 5 are reported in Table 4. Note that our gene clustering is assisted by the sample clustering in the biclustering framework, which is different from gene clustering methods that are only based on the correlation structure [4]. As a sanity check, the correlation matrix of the subset of the selected genes is plotted in Figure 13, and we can observe a clear pattern of block structure.

Table 4: Description or GenBank ID of the selected gene clusters of size at least 2 and at most 5

Cluster labels	Gene description/GenBank ID
(2, 7)	“proteoglycan 1, secretory granule”, “AI932613: Homo sapiens cDNA, 3 end”
(3, 4)	“AI147237: Homo sapiens cDNA, 3 end”, “S71043: Ig A heavy chain allotype 2”, “advanced glycosylation end product-specific receptor”, “leukocyte immunoglobulin-like receptor, subfamily B”
(5, 5)	“immunoglobulin lambda locus”, “glypican 3”
(5, 6)	“glutamate receptor, ionotropic, AMPA 2”, “small inducible cytokine subfamily A”, “W60864: Homo sapiens cDNA, 3 end”, “secreted phosphoprotein 1”, “LPS-induced TNF-alpha factor”
(6, 2)	“interleukin 6”, “carcinoembryonic antigen-related cell adhesion molecule 5”
(6, 11)	“secretory granule, neuroendocrine protein 1”, “alcohol dehydrogenase 2”, “neurofilament, light polypeptide”
(8, 3)	“fmaajor histocompatibility complex, class II”, “glycoprotein (transmembrane) nmb”
(8, 5)	“N90866: Homo sapiens cDNA, 3 end”, “receptor (calcitonin) activity modifying protein 1”

**Chicago crime data.** The Chicago crime data is publicly available at Chicago Police Department website<sup>4</sup>. The report in the website contains time, type, district, community area, latitude and longitude of each crime occurred. After removing missing data, we obtain 6.0 millions of crimes that occurred in 22 police districts from 2003 to 2018 (16 years). Here we restrict ourselves to the analysis of the spatial and temporal structure of Chicago crimes within the past few years, ignoring the types or categories of the crimes.

Since the 22 districts have different area sizes, we divide the total numbers of crimes in each district by its population density (population per unit area). We will call this quantity the *Chicago crime rate*. We observe that the Chicago crime rates exhibit decreasing patterns over the years. Since our study is focused on the relative comparisons among different police districts, we divide each entry by the sum of the yearly Chicago crime rates over all the 22 district in its current year. We will call this quantity the *relative crime rate*. Admittedly this preprocessing step does not reflect the difference between the *residential* and the *floating*

<sup>4</sup><https://data.cityofchicago.org/Public-Safety/Crimes-2001-to-present/>

populations in each district which might be important for the analysis of the crime data. For instance, around O’Hare international airport, it is very likely that the floating and the residential populations differ a lot. After the preprocessing, we obtain a three-way tensor with size  $22 \times 16 \times 4$ , for 22 districts, 16 years, and 4 seasons, which is visualized in Figure 14.

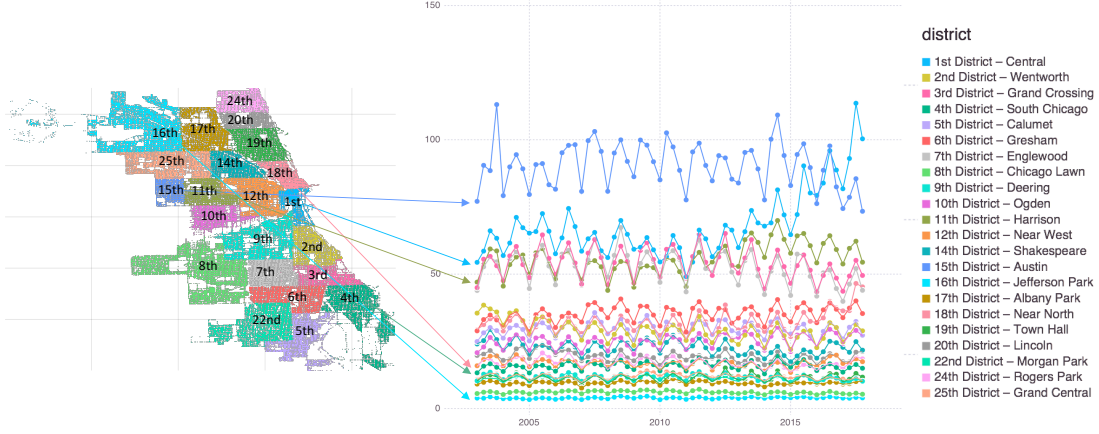


Figure 14: Visualization of the Chicago crime data after preprocessing.

Our main interest is to understand the geographical structure of the relative crime rates and how the structure changes over the year. A Bayesian model is constructed for this purpose by using the graphical tools under the proposed framework. We define a graph characterizing the geographical effect by  $G_1 = (V_1, E_1)$  with  $V_1 = \{1, 2, \dots, 22\}$  and  $E_1 = \{(i, j) : \text{the } i\text{th and } j\text{th districts are adjacent}\}$ . A graph characterizing the temporal effect is given by  $G_2 = (V_2, E_2)$  with  $V_2 = \{1, 2, \dots, 16\}$  and  $E_2 = \{(i, i + 1) : i = 1, \dots, 15\}$ . Then, the  $22 \times 16 \times 4$  tensor is modeled by a spike-and-slab Laplacian prior with the base graph  $G_1 \square G_2$ , in addition to a multivariate extension (Section 4.1) along the dimension of 4 seasons.

The result of the Bayesian model selection for the Chicago crime data is visualized in Figure 15. The geographical structure of the relative crime rates exhibit four different patterns according to the partition  $\{2003, 2004, \dots, 2015\}$ ,  $\{2016\}$ ,  $\{2017\}$ ,  $\{2018\}$ . While geographical compositions of the crimes are similar from 2003 to 2015, our results reveal that the last three years have witnessed dramatic changes. In particular, in these three years, the relative crime rates of Districts 11 and 15 were continuously decreasing, and the relative crime rates of Districts 1 and 18 show the opposite trend. This implies that the overall crime pattern is moving away from historically dangerous areas to downtown areas in Chicago.

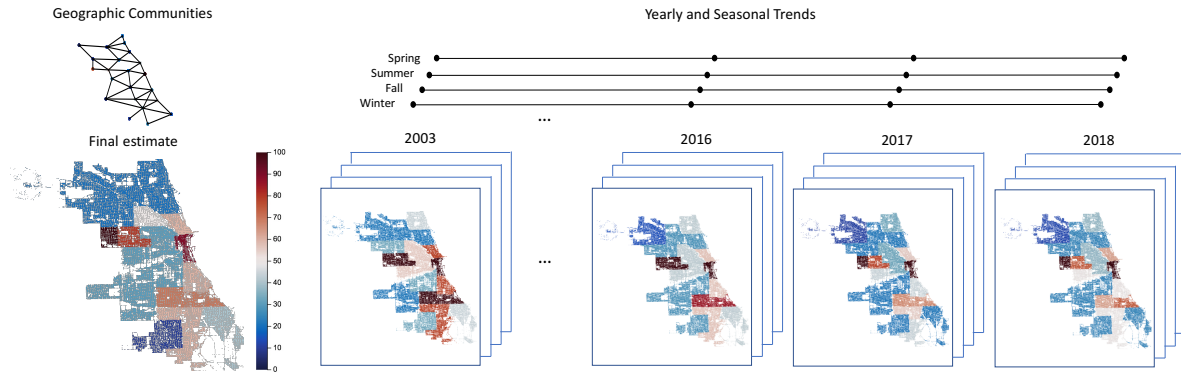


Figure 15: Visualization of Bayesian model selection for the Chicago crime data. (Left) The overall geographical pattern; (Right) Four different patterns from 2003 to 2018.

## References

- [1] Taylor B Arnold and Ryan J Tibshirani. *genlasso: Path algorithm for generalized lasso problems. R package version*, 1, 2014.
- [2] Andrew Barron, Lucien Birgé, and Pascal Massart. Risk bounds for model selection via penalization. *Probability theory and related fields*, 113(3):301–413, 1999.
- [3] Daniel Barry and John A Hartigan. A bayesian analysis for change point problems. *Journal of the American Statistical Association*, 88(421):309–319, 1993.
- [4] Arindam Bhattacharjee, William G Richards, Jane Staunton, Cheng Li, Stefano Monti, Priya Vasa, Christine Ladd, Javad Beheshti, Raphael Bueno, Michael Gillette, et al. Classification of human lung carcinomas by mrna expression profiling reveals distinct adenocarcinoma subclasses. *Proceedings of the National Academy of Sciences*, 98(24):13790–13795, 2001.
- [5] Leonard Bottolo and Sylvia Richardson. Evolutionary stochastic search for bayesian model exploration. *Bayesian Analysis*, 5(3):583–618, 2010.
- [6] Oleg Burdakov and Oleg Sysoev. A dual active-set algorithm for regularized monotonic regression. *Journal of Optimization Theory and Applications*, 172(3):929–949, 2017.
- [7] Yizong Cheng and George M Church. Biclustering of expression data. In *Ismb*, volume 8, pages 93–103, 2000.
- [8] Eric C Chi, Genevera I Allen, and Richard G Baraniuk. Convex biclustering. *Biometrics*, 73(1):10–19, 2017.
- [9] Patrick L Combettes and Jean-Christophe Pesquet. Proximal splitting methods in signal processing. In *Fixed-point algorithms for inverse problems in science and engineering*, pages 185–212. Springer, 2011.

- [10] Arthur P Dempster, Nan M Laird, and Donald B Rubin. Maximum likelihood from incomplete data via the em algorithm. *Journal of the royal statistical society. Series B (methodological)*, pages 1–38, 1977.
- [11] Jean Diebolt and Christian P Robert. Estimation of finite mixture distributions through bayesian sampling. *Journal of the Royal Statistical Society. Series B (Methodological)*, pages 363–375, 1994.
- [12] Richard L Dykstra. An algorithm for restricted least squares regression. *Journal of the American Statistical Association*, 78(384):837–842, 1983.
- [13] Zhou Fan and Leying and Guan. Approximate  $\ell_0$ -penalized estimation of piecewise-constant signals on graphs. *The Annals of Statistics*, 46(6B):3217–3245, 2018.
- [14] Uriel Feige and Robert Krauthgamer. Finding and certifying a large hidden clique in a semirandom graph. *Random Structures & Algorithms*, 16(2):195–208, 2000.
- [15] Felix Friedrich, Angela Kempe, Volkmar Liebscher, and Gerhard Winkler. Complexity penalized m-estimation: Fast computation. *Journal of Computational and Graphical Statistics*, 17(1):201–224, 2008.
- [16] Chao Gao, Aad W van der Vaart, and Harrison H Zhou. A general framework for bayes structured linear models. *arXiv preprint arXiv:1506.02174*, 2015.
- [17] Chao Gao, Fang Han, and Cun-Hui Zhang. On estimation of isotonic piecewise constant signals. *The Annals of Statistics*, to appear, 2018.
- [18] Edward I George and Robert E McCulloch. Variable selection via gibbs sampling. *Journal of the American Statistical Association*, 88(423):881–889, 1993.
- [19] Edward I George and Robert E McCulloch. Approaches for bayesian variable selection. *Statistica sinica*, pages 339–373, 1997.
- [20] Arpita Ghosh, Stephen Boyd, and Amin Saberi. Minimizing effective resistance of a graph. *SIAM review*, 50(1):37–66, 2008.
- [21] Joyee Ghosh and Merlise A Clyde. Rao-blackwellization for bayesian variable selection and model averaging in linear and binary regression: A novel data augmentation approach. *Journal of the American Statistical Association*, 106(495):1041–1052, 2011.
- [22] Bruce Hajek, Yihong Wu, and Jiaming Xu. Submatrix localization via message passing. *The Journal of Machine Learning Research*, 18(1):6817–6868, 2017.
- [23] Chris Hans, Adrian Dobra, and Mike West. Shotgun stochastic search for large p regression. *Journal of the American Statistical Association*, 102(478):507–516, 2007.
- [24] John A Hartigan. Direct clustering of a data matrix. *Journal of the american statistical association*, 67(337):123–129, 1972.

- [25] Wilfried Imrich and Sandi Klavzar. *Product graphs: structure and recognition*. Wiley, 2000.
- [26] Chinubhai G Khatri. Some results for the singular normal multivariate regression models. *Sankhyā: The Indian Journal of Statistics, Series A*, pages 267–280, 1968.
- [27] Mihee Lee, Haipeng Shen, Jianhua Z Huang, and JS Marron. Biclustering via sparse singular value decomposition. *Biometrics*, 66(4):1087–1095, 2010.
- [28] Jure Leskovec, Deepayan Chakrabarti, Jon Kleinberg, Christos Faloutsos, and Zoubin Ghahramani. Kronecker graphs: An approach to modeling networks. *Journal of Machine Learning Research*, 11(Feb):985–1042, 2010.
- [29] Fan Li and Nancy R Zhang. Bayesian variable selection in structured high-dimensional covariate spaces with applications in genomics. *Journal of the American statistical association*, 105(491):1202–1214, 2010.
- [30] Oren E Livne and Achi Brandt. Lean algebraic multigrid (lamg): Fast graph laplacian linear solver. *SIAM Journal on Scientific Computing*, 34(4):B499–B522, 2012.
- [31] László Lovász. Random walks on graphs: A survey. *Combinatorics, Paul erdos is eighty*, 2(1):1–46, 1993.
- [32] Zongming Ma and Yihong Wu. Volume ratio, sparsity, and minimaxity under unitarily invariant norms. *IEEE Transactions on Information Theory*, 61(12):6939–6956, 2015.
- [33] Patrick Mair, Kurt Hornik, and Jan de Leeuw. Isotone optimization in r: pool-adjacent-violators algorithm (pava) and active set methods. *Journal of statistical software*, 32(5): 1–24, 2009.
- [34] Toby J Mitchell and John J Beauchamp. Bayesian variable selection in linear regression. *Journal of the American Statistical Association*, 83(404):1023–1032, 1988.
- [35] Radford M Neal and Geoffrey E Hinton. A view of the em algorithm that justifies incremental, sparse, and other variants. In *Learning in graphical models*, pages 355–368. Springer, 1998.
- [36] Sylvia Richardson and Peter J Green. On bayesian analysis of mixtures with an unknown number of components (with discussion). *Journal of the Royal Statistical Society: series B (statistical methodology)*, 59(4):731–792, 1997.
- [37] Veronika Ročková and Edward I George. Emvs: The em approach to bayesian variable selection. *Journal of the American Statistical Association*, 109(506):828–846, 2014.
- [38] Michael J Schell and Bahadur Singh. The reduced monotonic regression method. *Journal of the American Statistical Association*, 92(437):128–135, 1997.

- [39] Yiyuan She. Sparse regression with exact clustering. *Electronic Journal of Statistics*, 4: 1055–1096, 2010.
- [40] Martin Sill, Sebastian Kaiser, Axel Benner, and Annette Kopp-Schneider. Robust biclustering by sparse singular value decomposition incorporating stability selection. *Bioinformatics*, 27(15):2089–2097, 2011.
- [41] Wang Songgui and Chow Shein-Chung. Advanced linear models: Theory and applications, 1994.
- [42] Daniel A Spielman. Spectral graph theory and its applications. In *Foundations of Computer Science, 2007. FOCS'07. 48th Annual IEEE Symposium on*, pages 29–38. IEEE, 2007.
- [43] Daniel A Spielman and Shang-Hua Teng. Nearly-linear time algorithms for graph partitioning, graph sparsification, and solving linear systems. In *Proceedings of the thirty-sixth annual ACM symposium on Theory of computing*, pages 81–90. ACM, 2004.
- [44] Terence Tao. *Topics in random matrix theory*, volume 132. American Mathematical Soc., 2012.
- [45] Robert Tibshirani, Michael Saunders, Saharon Rosset, Ji Zhu, and Keith Knight. Sparsity and smoothness via the fused lasso. *Journal of the Royal Statistical Society: Series B (Statistical Methodology)*, 67(1):91–108, 2005.
- [46] Ryan J Tibshirani and Jonathan Taylor. The solution path of the generalized lasso. *The Annals of Statistics*, 39(3):1335–1371, 2011.
- [47] Ryan J Tibshirani, Holger Hoeffling, and Robert Tibshirani. Nearly-isotonic regression. *Technometrics*, 53(1):54–61, 2011.
- [48] Martin J Wainwright and Michael I Jordan. Graphical models, exponential families, and variational inference. *Foundations and Trends® in Machine Learning*, 1(1–2):1–305, 2008.
- [49] Gao Wang, Abhishek K Sarkar, Peter Carbonetto, and Matthew Stephens. A simple new approach to variable selection in regression, with application to genetic fine-mapping. *bioRxiv*, page 501114, 2018.
- [50] Daniela M Witten and Robert Tibshirani. A framework for feature selection in clustering. *Journal of the American Statistical Association*, 105(490):713–726, 2010.
- [51] Wei Biao Wu, Michael Woodroffe, and Graciela Mentz. Isotonic regression: Another look at the changepoint problem. *Biometrika*, 88(3):793–804, 2001.

## A Some Basics on Linear Algebra

For a symmetric matrix  $\Gamma$  with rank  $r$ , it has an eigenvalue decomposition  $\Gamma = UDU^T$  with some orthonormal matrix  $U \in \mathcal{O}(p, r) = \{V \in \mathbb{R}^{p \times r} : V^T V = I_r\}$  and some diagonal matrix  $D$  whose diagonal entries are all positive. Then, the Moore-Penrose pseudo inverse of  $\Gamma$  is defined by

$$\Gamma^+ = UD^{-1}U^T.$$

**Lemma A.1.** *Consider a symmetric and invertible matrix  $R \in \mathbb{R}^{r \times r}$ . Then, we have*

$$R = V^T(VR^{-1}V^T)^+V, \quad (68)$$

for any  $V \in \mathcal{O}(p, r)$ .

*Proof.* To prove (68), we write  $R$  as its eigenvalue decomposition  $W\Lambda W^T$  for some  $W \in \mathcal{O}(r, r)$  and some invertible diagonal matrix  $\Lambda$ . Then, it is easy to see that  $VW \in \mathcal{O}(p, r)$ , and we thus have  $(VR^{-1}V^T)^+ = (VW\Lambda^{-1}W^TV^T)^+ = VW\Lambda W^TV^T$ , and then  $V^T(VR^{-1}V^T)^+V = V^TVW\Lambda W^TV^TV = W\Lambda W^T = R$ .  $\square$

**Lemma A.2.** *Let  $A, B \in \mathbb{R}^{n \times m}$  be matrices of full column rank  $m$  (i.e.  $m \leq n$ ). Let  $Z_A$  and  $Z_B$  span the nullspaces of  $A$  and  $B$ , respectively. That is,  $Z_A, Z_B \in \mathbb{R}^{n \times (n-m)}$  and*

$$A^T Z_A = 0, \quad B^T Z_B = 0.$$

Then, we have

$$I_n - A(B^T A)^{-1}B^T = Z_B(Z_A^T Z_B)^{-1}Z_A^T.$$

*Proof.* Let  $C = I_n - A(B^T A)^{-1}B^T$ , and then it is easy to check that

$$CZ_B = Z_B, \quad Z_A^T C = Z_A^T, \quad CA = 0, \quad B^T C = 0.$$

Note that the above four equations determine the singular value decomposition of  $C$  and are also satisfied by  $Z_B(Z_A^T Z_B)^{-1}Z_A^T$ , which immediately implies  $C = Z_B(Z_A^T Z_B)^{-1}Z_A^T$ .  $\square$

**Lemma A.3.** *Suppose for symmetric matrices  $S, H \in \mathbb{R}^{p \times p}$ , we have  $\mathcal{M}([S; H]) = \mathbb{R}^p$ , where the notation  $\mathcal{M}(\cdot)$  means the subspace spanned by the columns of a matrix. Then, we have*

$$(tS + H)^{-1} \rightarrow R(R^T H R)^{-1}R^T,$$

as  $t \rightarrow \infty$ , where  $R$  is any matrix such that  $\mathcal{M}(R)$  is the null space of  $S$ .

*Proof.* We first prove the special case of  $H = I_p$ . Denote the rank of  $S$  by  $r$ , and then  $S$  has an eigenvalue decomposition  $S = UDU^T$  for some  $U \in \mathcal{O}(p, r)$  and some diagonal matrix  $D$  with positive diagonal entries. Since  $\mathcal{M}(R)$  is the null space of  $S$ , we have  $I_p = UU^T + R(R^T R)^{-1}R^T$  by Lemma A.2. Then,

$$(tS + I_p)^{-1} = (U(tD + I_r)U^T + R(R^T R)^{-1}R^T)^{-1} = U(tD + I_r)^{-1}U^T + R(R^T R)^{-1}R^T,$$

which converges to  $R(R^T R)^{-1} R^T$  as  $t \rightarrow \infty$ . The second equality above follows from  $U^T R = 0$ . Now we assume a general  $H$  of full rank, which means  $H = Q^T Q$  for some  $Q \in \mathbb{R}^{p \times p}$  that is invertible. Then,

$$(tS + H)^{-1} = Q^{-1}(t(Q^T)^{-1} S Q^{-1} + I_p)^{-1} (Q^T)^{-1}.$$

Since the null space of  $(Q^T)^{-1} S Q^{-1}$  is  $\mathcal{M}(QR)$ , we have

$$(t(Q^T)^{-1} S Q^{-1} + I_p)^{-1} \rightarrow QR(R^T Q^T QR)^{-1} R^T Q^T = QR(R^T H R)^{-1} R^T Q^T,$$

and therefore  $(tS + H)^{-1} \rightarrow R(R^T H R)^{-1} R^T$ . For a general  $H$  that is not necessarily full rank, since  $\mathcal{M}([S; H]) = \mathbb{R}^p$ ,  $S + H$  is a matrix of full rank. Then,

$$(tS + H)^{-1} = ((t-1)S + S + H)^{-1} \rightarrow R(R^T(S + H)R)^{-1} R^T = R(R^T H R)^{-1} R^T,$$

and the proof is complete.  $\square$

## B Degenerate Gaussian Distributions

A multivariate Gaussian distribution is fully characterized by its mean vector and covariance matrix. For  $N(\mu, \Sigma)$  with some  $\mu \in \mathbb{R}^p$  and a positive semidefinite  $\Sigma \in \mathbb{R}^{p \times p}$ , we call the distribution degenerate if  $\text{rank}(\Sigma) < p$ . Given any  $\Sigma$  such that  $\text{rank}(\Sigma) = r < p$ , we have the decomposition  $\Sigma = AA^T$  for some  $A \in \mathbb{R}^{p \times r}$ . Therefore,  $X \sim N(\mu, \Sigma)$  if and only if

$$X = \mu + AZ, \tag{69}$$

where  $Z \sim N(0, I_r)$ . The latent variable representation (69) immediately implies that  $X - \mu \in \mathcal{M}(A) = \mathcal{M}(\Sigma)$  with probability one.

The density function of  $N(\mu, \Sigma)$  is given by

$$(2\pi)^{-r/2} \frac{1}{\sqrt{\det_+(\Sigma)}} \exp\left(-\frac{1}{2}(x - \mu)^T \Sigma^+ (x - \mu)\right) \mathbb{I}\{x - \mu \in \mathcal{M}(\Sigma)\}. \tag{70}$$

The formula (70) can be found in [26, 41]. Note that the density function (70) is defined with respect to the Lebesgue measure on the subspace  $\{x : x - \mu \in \mathcal{M}(\Sigma)\}$ . Here, the  $\det_+(\cdot)$  is used for the product of all nonzero eigenvalues of a symmetric matrix, and  $\Sigma^+$  is the Moore-Penrose inverse of the covariance matrix  $\Sigma$ . The two characterizations (69) and (70) of  $N(\mu, \Sigma)$  are equivalent to each other.

The property is useful for us to identify whether a formula leads to a well-defined density function of a degenerate Gaussian distribution.

**Lemma B.1.** *Suppose  $f(x) = \exp(-\frac{1}{2}(x - \mu)^T \Omega (x - \mu)) \mathbb{I}\{x - \mu \in \mathcal{M}(V)\}$  for some  $\mu \in \mathbb{R}^p$ , some positive semidefinite  $\Omega \in \mathbb{R}^{p \times p}$  and some  $V \in \mathcal{O}(p, r)$ . As long as  $\mathcal{M}(\Omega V) = \mathcal{M}(V)$ , we have  $\int f(x) dx < \infty$ , and  $f(x) / \int f(x) dx$  is the density function of  $N(\mu, \Sigma)$  with  $\Sigma = V(V^T \Omega V)^{-1} V^T$ .*

*Proof.* Without loss of generality, assume  $\mu = 0$ . Since  $\mathcal{M}(\Omega V) = \mathcal{M}(V)$ ,  $V^T \Omega V$  is an invertible matrix, and thus  $\Sigma$  is well defined. It is easy to see that  $\mathcal{M}(V) = \mathcal{M}(\Sigma)$ . Therefore, in view of (70), we only need to show

$$x^T \Omega x = x^T (V(V^T \Omega V)^{-1} V^T)^+ x,$$

for all  $x \in \mathcal{M}(V)$ . Since  $x = VV^T x$  for all  $x \in \mathcal{M}(V)$ , it suffices to show

$$V^T \Omega V = V^T (V(V^T \Omega V)^{-1} V^T)^+ V,$$

which is immediately implied by (68) with  $R = V^T \Omega V$ . The proof is complete.  $\square$

We remark that Lemma B.1 also holds for a  $V \in \mathbb{R}^{p \times r}$  that satisfies  $\text{rank}(V) = r$  but is not necessarily orthonormal. This is because  $V(V^T \Omega V)^{-1} V^T = W(W^T \Omega W)^{-1} W^T$  whenever  $\mathcal{M}(V) = \mathcal{M}(W)$ .

## C Proofs of Propositions

*Proof of Proposition 2.1.* The property of the Laplacian matrix  $L_\gamma$  is standard in spectral graph theory [42]. We apply Lemma B.1 with  $\mu = 0$ ,  $\Omega = \sigma^{-2} L_\gamma$  and  $V$  is chosen arbitrarily from  $\mathcal{O}(p, p-1)$  such that  $w^T V = 0$ . Then, the condition  $\mathcal{M}(\Omega V) = \mathcal{M}(V)$  is equivalent to  $\mathbb{1}_p^T w \neq 0$ , because  $\mathbb{1}_p$  spans the null space of  $L_\gamma$ . Note that (68) immediately implies  $VRV^T = VV^T(VR^{-1}V^T)^+ VV^T = (VR^{-1}V^T)^+$ . We then have

$$\begin{aligned} \det_+(V(V^T \Omega V)^{-1} V^T) &= \sigma^{2(p-1)} \det_+(V(V^T L_\gamma V)^{-1} V^T) \\ &= \sigma^{2(p-1)} \det_+((VV^T L_\gamma VV^T)^+) \\ &= \sigma^{2(p-1)} \frac{1}{\det_+(VV^T L_\gamma VV^T)}. \end{aligned}$$

The proof is complete by realizing that  $VV^T = I_p - ww^T/\|w\|^2$  from Lemma A.2.  $\square$

*Proof of Proposition 3.1.* Recall the incidence matrix  $D \in \mathbb{R}^{m \times p}$  defined in Section 2.1. With the new notations  $\Phi = D^T \text{diag}(\gamma)D$  and  $\Psi = D^T \text{diag}(1 - \gamma)D$ , we can write  $L_\gamma = v_0^{-1} \Phi + v_1^{-1} \Psi$  and  $\tilde{L}_\gamma = v_1^{-1} \Psi$ .

We first prove that (22) is well defined. By Lemma B.1, it is sufficient to show  $\tilde{V}^T Z_\gamma^T \Psi Z_\gamma \tilde{V}$  is invertible. This is because  $\mathcal{M}([\Phi; \Psi; w]) = \mathbb{R}^p$ , and the columns of  $Z_\gamma \tilde{V}$  are all orthogonal to  $\mathcal{M}([\Phi; w])$ . Therefore, (22) is well defined and its covariance matrix is given by (71).

Now we will show the distribution (8) converges to that of  $Z_\gamma \tilde{\theta}$  with  $\tilde{\theta}$  distributed by (22) as  $v_0 \rightarrow 0$ . Let  $\tilde{V} \in \mathbb{R}^{r \times r-1}$  be a matrix of rank  $r-1$  that satisfies  $\tilde{V}^T Z_\gamma^T w = 0$ . Then, by Lemma B.1, the distribution (22) can be written as

$$\tilde{\theta} \sim N(0, \sigma^2 \tilde{V} (\tilde{V}^T Z_\gamma^T \tilde{L}_\gamma Z_\gamma \tilde{V})^{-1} \tilde{V}^T), \quad (71)$$

which implies

$$Z_\gamma \tilde{\theta} \sim N(0, \sigma^2 Z_\gamma \tilde{V} (\tilde{V}^T Z_\gamma^T \tilde{L}_\gamma Z_\gamma \tilde{V})^{-1} \tilde{V}^T Z_\gamma^T).$$

On the other hand, the distribution (8) can be written as

$$\theta \sim N(0, \sigma^2 V(V^T L_\gamma V)^{-1} V^T),$$

where the matrix  $V \in \mathbb{R}^{p \times p-1}$  can be chosen to be any matrix of rank  $p-1$  that satisfies  $V^T w = 0$ . In particular, we can choose  $V$  that takes the form of

$$V = [Z_\gamma \tilde{V}; U],$$

where  $U \in \mathcal{O}(p, p-r)$  and  $U$  satisfies  $U^T w = 0$  and  $U^T Z_\gamma \tilde{V} = 0$ . Since both  $\theta$  and  $Z_\gamma \tilde{\theta}$  are Gaussian random vectors, we need to prove

$$V(V^T L_\gamma V)^{-1} V^T \rightarrow Z_\gamma \tilde{V} (\tilde{V}^T Z_\gamma^T \tilde{L}_\gamma Z_\gamma \tilde{V})^{-1} \tilde{V}^T Z_\gamma^T, \quad (72)$$

as  $v_0 \rightarrow 0$ . Note that (72) is equivalent to

$$V(v_0^{-1} V^T \Phi V + v_1^{-1} V^T \Psi V)^{-1} V^T \rightarrow v_1 Z_\gamma \tilde{V} (\tilde{V}^T Z_\gamma^T \Psi Z_\gamma \tilde{V})^{-1} \tilde{V}^T Z_\gamma^T, \quad (73)$$

as  $v_0 \rightarrow 0$ . By the definition of  $Z_\gamma$  and the property of graph Laplacian, the null space of  $\Phi$  is  $\mathcal{M}(Z_\gamma)$ . By the construction of  $V$ , the null space of  $V^T \Phi V$  is  $\mathcal{M}(V^T Z_\gamma)$ . Moreover, we have  $\mathcal{M}([V^T \Phi V; V^T \Psi V]) = \mathbb{R}^{p-1}$ . Therefore, Lemma A.3 implies that

$$(v_0^{-1} V^T \Phi V + v_1^{-1} V^T \Psi V)^{-1} \rightarrow v_1 V^T Z_\gamma (Z_\gamma^T V V^T \Psi V V^T Z_\gamma)^{-1} Z_\gamma^T V,$$

and thus

$$V(v_0^{-1} V^T \Phi V + v_1^{-1} V^T \Psi V)^{-1} V^T \rightarrow v_1 V V^T Z_\gamma (Z_\gamma^T V V^T \Psi V V^T Z_\gamma)^{-1} Z_\gamma^T V V^T.$$

Since  $V V^T Z_\gamma = Z_\gamma \tilde{V} \tilde{V}^T Z_\gamma^T Z_\gamma$ , we have  $\mathcal{M}(V V^T Z_\gamma) = \mathcal{M}(Z_\gamma \tilde{V})$ . This implies

$$V V^T Z_\gamma (Z_\gamma^T V V^T \Psi V V^T Z_\gamma)^{-1} Z_\gamma^T V V^T = Z_\gamma \tilde{V} (\tilde{V}^T Z_\gamma^T \Psi Z_\gamma \tilde{V})^{-1} \tilde{V}^T Z_\gamma^T,$$

and therefore we obtain (73). The proof is complete.  $\square$

*Proof of Proposition 4.1.* We only prove the case with  $d = 1$ . The general case with  $d \geq 2$  follows the same argument with more complicated notation of covariance matrices (such as Kronecker products). By Lemma B.1, (30) is the density function of  $N(0, \Sigma)$ , with

$$\Sigma = \sigma^2 U(U^T L_\gamma U)^{-1} U^T,$$

where

$$L_\gamma = \begin{bmatrix} (v_0^{-1} - v_1^{-1})I_n + v_1^{-1}kI_n & -(v_0^{-1} - v_1^{-1})\gamma - v_1^{-1}\mathbf{1}_{n \times k} \\ -(v_0^{-1} - v_1^{-1})\gamma^T - v_1^{-1}\mathbf{1}_{k \times n} & (v_0^{-1} - v_1^{-1})\gamma^T \gamma + v_1^{-1}nI_k \end{bmatrix}.$$

The matrix  $U$  is defined by

$$U = \begin{bmatrix} V & 0_{n \times k} \\ 0_{k \times (n-1)} & I_k \end{bmatrix},$$

and  $V \in \mathbb{R}^{n \times (n-1)}$  is a matrix of rank  $n-1$  that satisfies  $\mathbf{1}_n^T V = 0$ . Note that  $\theta|\gamma, \sigma^2$  follows  $N(0, \Sigma_{[n] \times [n]})$ . That is, the covariance matrix is the top  $n \times n$  submatrix of  $\Sigma$ . A direct calculation gives

$$\Sigma_{[n] \times [n]} = \sigma^2 V [V^T (A - BC^{-1}B^T) V]^{-1} V^T,$$

where

$$\begin{aligned} A &= (v_0^{-1} - v_1^{-1})I_n + v_1^{-1}kI_n, \\ B &= -(v_0^{-1} - v_1^{-1})\gamma - v_1^{-1}\mathbf{1}_{n \times k}, \\ C &= (v_0^{-1} - v_1^{-1})\gamma^T \gamma + v_1^{-1}nI_k. \end{aligned}$$

Letting  $v_1 \rightarrow \infty$ , we have

$$\Sigma_{[n] \times [n]} \rightarrow \sigma^2 v_0 V [V^T (I_n - \gamma(\gamma^T \gamma)^{-1} \gamma^T) V]^{-1} V^T.$$

The existence of  $(\gamma^T \gamma)^T$  is guaranteed by the condition that  $\gamma$  is non-degenerate. By Lemma B.1,  $p(\theta|\gamma, \sigma^2) \propto \prod_{1 \leq i < l \leq n} \exp\left(-\frac{\lambda_{il} \|\theta_i - \theta_l\|^2}{2\sigma^2 v_0}\right) \mathbb{I}\{\mathbf{1}_n^T \theta = 0\}$  is the density function of  $N(0, \sigma^2 v_0 V [V^T (I_n - \gamma(\gamma^T \gamma)^{-1} \gamma^T) V]^{-1} V^T)$ , which completes the proof.  $\square$

*Proof of Proposition 4.2.* We only prove the case with  $d = 1$ . The general case with  $d \geq 2$  follows the same argument with more complicated notation of covariance matrices (such as Kronecker products). The proof is basically an application of Proposition 3.1. That is, as  $v_0 \rightarrow 0$ , the distribution of  $(\theta^T, \mu^T)^T$  weakly converges to that of  $Z_\gamma \tilde{\mu}$ . In the current setting, we have

$$Z_\gamma = \begin{bmatrix} \gamma \\ I_k \end{bmatrix}.$$

The random vector  $\tilde{\mu}$  is distributed by (23). Note that the contracted base graph is a complete graph on  $\{1, \dots, k\}$ , and  $w_{jl} = n_j + n_l$  in the current setting. The density (23) thus becomes

$$p(\tilde{\mu}|\gamma, \sigma^2) \propto \prod_{1 \leq j < l \leq k} \exp\left(-\frac{(n_j + n_l)(\tilde{\mu}_j - \tilde{\mu}_l)^2}{2\sigma^2 v_1}\right) \mathbb{I}\{\mathbf{1}_n^T \gamma \tilde{\mu} = 0\}.$$

Finally, the relations  $\theta = \gamma \tilde{\mu}$  and  $\mu = \tilde{\mu}$  lead to the desired conclusion.  $\square$

*Proof of Proposition 6.1.* Note that the integration is with respect to the Lebesgue measure on the  $(n-1)$ -dimensional subspace  $\{\theta : \mathbf{1}_n^T \theta = 0\}$ . Consider a matrix  $V \in \mathbb{R}^{n \times n-1}$  of rank  $n-1$  that satisfies  $\mathbf{1}_n^T V = 0$ , which means that the columns of  $[\mathbf{1}_n : V] \in \mathbb{R}^{n \times n}$  form a nondegenerate basis. Then, we can write  $d\theta$  in the integral as  $\frac{1}{\sqrt{\det(V^T V)}} d(V^T \theta)$ . For the Laplacian matrix  $L_\gamma$  that satisfies  $\theta^T L_\gamma \theta = \sum_{i=1}^{n-1} \frac{(\theta_{i+1} - \theta_i)^2}{v_0 \gamma_i + v_1 (1 - \gamma_i)}$ , we have  $\mathbf{1}_n^T L_\gamma = 0$ . In particular, we choose  $V$  such that its  $i$ th column is  $V_{*i} = e_i - e_{i+1}$ , where  $e_i$  is a vector whose  $i$ th entry is 1 and 0 elsewhere. Then, we have  $L_\gamma = V S_\gamma V^T$  with  $S_\gamma = \text{diag}(v_0^{-1} \gamma + v_1^{-1} (1 - \gamma))$ ,

and the integral becomes

$$\begin{aligned}
& \int_{\mathbf{1}_n^T \theta = 0, \theta_1 \leq \dots \leq \theta_n} 2^{(n-1)} \frac{1}{(2\pi\sigma^2)^{(n-1)/2}} \sqrt{\det_{\mathbf{1}_n}(L_\gamma)} \exp\left(-\frac{1}{2\sigma^2} \theta^T L_\gamma \theta\right) d\theta \\
&= \int_{\theta_1 \leq \dots \leq \theta_n} 2^{(n-1)} \frac{1}{(2\pi\sigma^2)^{(n-1)/2}} \sqrt{\frac{\det_{\mathbf{1}_n}(L_\gamma)}{\det(V^T V)}} \exp\left(-\frac{1}{2\sigma^2} \theta^T V S_\gamma V^T \theta\right) d(V^T \theta) \\
&= \int_{\delta_1 \leq 0, \dots, \delta_n \leq 0} 2^{(n-1)} \frac{1}{(2\pi\sigma^2)^{(n-1)/2}} \sqrt{\frac{\det_{\mathbf{1}_n}(L_\gamma)}{\det(V^T V)}} \exp\left(-\frac{1}{2\sigma^2} \delta^T S_\gamma \delta\right) d\delta \\
&= \int \frac{1}{(2\pi\sigma^2)^{(n-1)/2}} \sqrt{\frac{\det_{\mathbf{1}_n}(L_\gamma)}{\det(V^T V)}} \exp\left(-\frac{1}{2\sigma^2} \delta^T S_\gamma \delta\right) d\delta \tag{74} \\
&= \sqrt{\frac{\det_{\mathbf{1}_n}(L_\gamma)}{\det(S_\gamma) \det(V^T V)}} \tag{75} \\
&= 1,
\end{aligned}$$

where the last equality is by  $\det_{\mathbf{1}_n}(L_\gamma) = \det_+(V S_\gamma V^T) = \det(S_\gamma) \det(V^T V)$ . The equality (74) is by the symmetry of  $\exp\left(-\frac{1}{2\sigma^2} \delta^T S_\gamma \delta\right)$ , and (75) is by Lemma B.1. Finally, Lemma 3.1 says that

$$\det_{\mathbf{1}_n}(L_\gamma) = n \prod_{i=1}^{n-1} [v_0^{-1} \gamma_i + v_1^{-1} (1 - \gamma_i)]$$

This completes the proof.  $\square$

*Proof of Proposition 6.2.* We need to calculate

$$\int_{\mathbf{1}_n^T Z_\gamma \tilde{\theta} = 0, \tilde{\theta}_1 \leq \dots \leq \tilde{\theta}_s} \prod_{l=1}^s \exp\left(-\frac{(\tilde{\theta}_l - \tilde{\theta}_{l+1})^2}{2\sigma^2 v_1}\right) d\tilde{\theta},$$

where the integral is taken with respect to the Lebesgue measure on the low-dimensional subspace  $\{\tilde{\theta} : \mathbf{1}_n^T Z_\gamma \tilde{\theta} = 0\}$ . Choose  $\tilde{V}_{*l} = e_l - e_{l+1}$ , where  $e_l \in \{0, 1\}^s$  is a vector whose  $l$ th entry is 1 and 0 elsewhere. Then the columns of  $[Z_\gamma^T \mathbf{1}_n : (Z_\gamma^T Z_\gamma)^{-1} \tilde{V}] \in \mathbb{R}^{s \times s}$  form a non-degenerate basis of  $\mathbb{R}^s$ . This is because

$$Z_\gamma^T \mathbf{1}_n = (n_1, \dots, n_s)^T, \quad Z_\gamma^T Z_\gamma = \text{diag}(n_1, \dots, n_s),$$

where  $n_l$  is the size of  $l$ th cluster. Furthermore,  $Z_\gamma^T \mathbf{1}_n$  and  $(Z_\gamma^T Z_\gamma)^{-1} \tilde{V}$  are orthogonal to

each other. We write  $\widetilde{W} = (Z_\gamma^T Z_\gamma)^{-1} \widetilde{V}$  for simplicity. Then,

$$\begin{aligned}
& \int_{\mathbf{1}_n^T Z_\gamma \widetilde{\theta} = 0, \widetilde{\theta}_1 \leq \dots \leq \widetilde{\theta}_s} \prod_{l=1}^s \exp \left( -\frac{(\widetilde{\theta}_l - \widetilde{\theta}_{l+1})^2}{2\sigma^2 v_1} \right) d\widetilde{\theta} \\
&= \frac{1}{\sqrt{\det \widetilde{W}^T \widetilde{W}}} \int_{\widetilde{\theta}_1 \leq \dots \leq \widetilde{\theta}_s} \prod_{l=1}^s \exp \left( -\frac{(\widetilde{\theta}_l - \widetilde{\theta}_{l+1})^2}{2\sigma^2 v_1} \right) d(\widetilde{W}^T \widetilde{\theta}) \\
&= \frac{\det \widetilde{W}^T \widetilde{W} (\widetilde{V}^T \widetilde{W})^{-1}}{\sqrt{\det \widetilde{W}^T \widetilde{W}}} \int_{\widetilde{\theta}_1 \leq \dots \leq \widetilde{\theta}_s} \prod_{l=1}^{s-1} \exp \left( -\frac{(\widetilde{\theta}_l - \widetilde{\theta}_{l+1})^2}{2\sigma^2 v_1} \right) d(\widetilde{V}^T \widetilde{\theta}) \\
&= \frac{\det \widetilde{W}^T \widetilde{W} (\widetilde{V}^T \widetilde{W})^{-1}}{\sqrt{\det \widetilde{W}^T \widetilde{W}}} \int_{\widetilde{\delta}_1, \dots, \widetilde{\delta}_{s-1} \leq 0} \prod_{l=1}^{s-1} \exp \left( -\frac{\widetilde{\delta}_l^2}{2\sigma^2 v_1} \right) d\widetilde{\delta} \\
&= \frac{\sqrt{\det \widetilde{W}^T \widetilde{W}}}{\det \widetilde{V}^T \widetilde{W}} \int_{\widetilde{\delta}_1, \dots, \widetilde{\delta}_{s-1} \leq 0} \prod_{l=1}^{s-1} \exp \left( -\frac{\widetilde{\delta}_l^2}{2\sigma^2 v_1} \right) d\widetilde{\delta} \\
&= \frac{(2\pi\sigma^2 v_1)^{(s-1)/2}}{2^{s-1}} \times \frac{\sqrt{\det \widetilde{W}^T \widetilde{W}}}{\det \widetilde{V}^T \widetilde{W}}.
\end{aligned}$$

The first equality is from the Lebesgue integration on the reduced space and the last equality is by symmetry. The second equality follows from the change of variables formula, because for any  $\widetilde{\theta}$  such that  $\mathbf{1}_n^T Z_\gamma \widetilde{\theta} = 0$ ,  $\widetilde{\theta} = \widetilde{W}U$  for some  $U$ , which leads to  $\widetilde{W}^T \widetilde{W} (\widetilde{V}^T \widetilde{W})^{-1} \widetilde{V}^T \widetilde{\theta} = \widetilde{W}^T \widetilde{W} U = \widetilde{W}^T \widetilde{\theta}$ . Finally, we observe that

$$v_1^{(s-1)/2} \sqrt{\det_{Z_\gamma^T \mathbf{1}_n} (Z_\gamma^T \widetilde{L}_\gamma Z_\gamma)} = \left( \frac{\det(\widetilde{W}^T \widetilde{V} \widetilde{V}^T \widetilde{W})}{\det \widetilde{W}^T \widetilde{W}} \right)^{1/2} = \left( \frac{(\det \widetilde{V}^T \widetilde{W})^2}{\det \widetilde{W}^T \widetilde{W}} \right)^{1/2} = \frac{\det \widetilde{V}^T \widetilde{W}}{\sqrt{\det \widetilde{W}^T \widetilde{W}}},$$

since  $\widetilde{V} \widetilde{V}^T = v_1 \widetilde{L}_\gamma$  is the reduced graph Laplacian and the columns of  $\widetilde{W}$  spans the nullspace of  $Z_\gamma^T \mathbf{1}_n$ . The proof is complete.  $\square$

## D Proof of Lemma 3.1

We let  $U \in \mathcal{O}(p, p-1)$  be an orthonormal matrix that satisfies  $\mathbf{1}_p^T U = 0$ , and  $V \in \mathcal{O}(p, p-1)$  be an orthonormal matrix that satisfies  $w^T V = 0$ . Write  $I_p - U(V^T U)^{-1} V^T$  as  $R$ . Then,  $RU = 0$ , which implies that  $R$  has rank at most one. The facts  $Rw = w$  and  $\mathbf{1}_p^T R = \mathbf{1}_p^T$ , together with Lemma A.2, imply that

$$I_p - U(V^T U)^{-1} V^T = \frac{1}{\mathbf{1}_p^T w} w \mathbf{1}_p^T. \quad (76)$$

Therefore,

$$\begin{aligned}
\det_w(L_\gamma) &= \det_+(V V^T L_\gamma V V^T) \\
&= \det(V^T L_\gamma V) \\
&= \det(V^T U U^T L_\gamma U U^T V) \\
&= (\det(V^T U))^2 \det(U^T L_\gamma U).
\end{aligned} \quad (77)$$

The inequality (77) is because  $UU^T$  is a projection matrix to the null space of  $L_\gamma$ . We are going to calculate  $\det(V^T U)$  and  $\det(U^T L_\gamma U)$  separately. For  $\det(V^T U)$ , we have

$$\begin{aligned}
1 &= \det \left( \begin{bmatrix} V & \|w\|^{-1} w \end{bmatrix}^T \begin{bmatrix} U & p^{-1/2} \mathbf{1}_p \end{bmatrix} \right) \\
&= \det \left( \begin{bmatrix} V^T U & p^{-1/2} V^T \mathbf{1}_p \\ \|w\|^{-1} w^T U & w^T \mathbf{1}_p / (p^{1/2} \|w\|) \end{bmatrix} \right) \\
&= \det(V^T U) \det(w^T (I_p - U(V^T U)^{-1} V^T) \mathbf{1}_p) / (p^{1/2} \|w\|) \\
&= \det(V^T U) \frac{p^{1/2} \|w\|}{\mathbf{1}_p^T w},
\end{aligned}$$

and we thus get

$$(\det(V^T U))^2 = \frac{(\mathbf{1}_p^T w)^2}{p \|w\|^2}. \quad (78)$$

We use (76) for the equality (78).

The calculation of  $\det(U^T L_\gamma U)$  requires the Cauchy-Binet formula. For any given matrices  $A, B \in \mathbb{R}^{n \times m}$  with  $n \leq m$ , we have

$$\det(AB^T) = \sum_{\{S \subset [m]: |S|=n\}} \det(B_{*S}^T A_{*S}). \quad (79)$$

The version (79) can be found in [44]. Let  $A = B = U^T D^T (v_0^{-1/2} \text{diag}(\gamma) + v_1^{-1/2} \text{diag}(1 - \gamma))$ , and we have

$$\det(U^T L_\gamma U) = \sum_{\{S \subset E: |S|=p-1\}} \left( \prod_{(i,j) \in S} [v_0^{-1} \gamma_{ij} + v_1^{-1} (1 - \gamma_{ij})] \right) \det(D_{S*} U U^T D_{S*}^T).$$

Note that  $\det(D_{S*} U U^T D_{S*}^T) = \det(U^T D_{S*}^T D_{S*} U)$ , and  $D_{S*}^T D_{S*}$  is the graph Laplacian of a subgraph of the base graph with the edge set  $S$ . Since  $|S| = p - 1$ ,  $S$  is either a spanning tree ( $\det(U^T D_{S*}^T D_{S*} U) = p$ ) or is disconnected ( $\det(U^T D_{S*}^T D_{S*} U) = 0$ ), we have

$$\det(U^T L_\gamma U) = p \sum_{T \in \text{spt}(G)} \prod_{(i,j) \in T} [v_0^{-1} \gamma_{ij} + v_1^{-1} (1 - \gamma_{ij})]. \quad (80)$$

Therefore, by plugging (78) and (80) into (77), we obtain the desired conclusion.

## E Some Implementation Details

In this section, we present a fast algorithm that solves the M-step (54). To simplify the notation in the discussion, we consider a special case with  $X_1 = I_{n_1}$ ,  $X_2 = I_{n_2}$ ,  $w = \mathbf{1}_{n_1} \mathbf{1}_{n_2}^T$

---

**Algorithm 1:** A fast DLPA

---

Initialize  $u_1, u_2$  and  $z_2$ .

**while** *before convergence* **do**

$$\left| \begin{array}{l} z_1^{new} = (I_{n_1} + L_{q_1})^{-1}(z_2 + u_2), \quad z_2^{new} = (z_1^{new} + u_1)(I_{n_2} + L_{q_2})^{-1} \\ u_1^{new} = z_2 + u_2 - z_1^{new}, \quad u_2^{new} = z_1^{new} + u_2 - z_2^{new} \\ z_1 = z_1^{new}, \quad z_2 = z_2^{new}, \quad u_1 = u_1^{new}, \quad u_2 = u_2^{new} \end{array} \right.$$

**end**

**return**  $\theta = z_2$

---

and  $\nu = 0$ , which is the most important setting that we need for the biclustering problem. In other words, we need to optimize  $F(\theta; q_1, q_2)$  over  $\theta \in \Theta_w$  for any  $q_1$  and  $q_2$ , where

$$F(\theta; q_1, q_2) = \|y - \bar{y}\mathbf{1}_{n_1}\mathbf{1}_{n_2}^T - \theta\|_F^2 + \text{vec}(\theta)^T (L_{q_2} \otimes I_{p_1} + I_{p_2} \otimes L_{q_1}) \text{vec}(\theta) \quad (81)$$

$$= \|y - \bar{y}\mathbf{1}_{n_1}\mathbf{1}_{n_2}^T - \theta\|_F^2 + \langle \theta\theta^T, L_{q_1} \rangle + \langle \theta^T\theta, L_{q_2} \rangle. \quad (82)$$

Algorithm 1 is a Dykstra-like proximal algorithm (DLPA) [12] that iteratively solves the optimization problem. It is shown that Algorithm 1 has a provable linear convergence [9]. If we initialize  $u_1 = u_2 = 0_{n_1 \times n_2}$  and  $z_2 = y - \bar{y}\mathbf{1}_{n_1}\mathbf{1}_{n_2}^T$  with  $\hat{\alpha} = \bar{y}$ , then the first two steps of Algorithm 1 can be written as the following update

$$\theta^{new} = (I_{n_1} + L_{q_1})^{-1} (y - \bar{y}\mathbf{1}_{n_1}\mathbf{1}_{n_2}^T) (I_{n_2} + L_{q_2})^{-1}. \quad (83)$$

In practice, we suggest using (83) as approximate M-step updates in the first few iterations of the EM algorithm. Then, the full version of Algorithm 1 can be implemented in later iterations to ensure convergence.